NASA TECHNICAL NOTE

NASA TN D-6397

NASA TN D-6397

STATIC AERODYNAMIC CHARACTERISTICS OF A SCOUT FIN WITH AN ENLARGED TIP CONTROL AT MACH NUMBERS FROM 0.40 TO 4.63

by

Robert J. Keynton
Langley Research Center

and

Thomas G. Muir
LTV Aerospace Corporation

NATIONAL AERONAUTICS AND SPACE ADMINISTRATION • WASHINGTON, D. C. • SEPTEMBER 1971

1. Report No.	2. Government Accession No.	3. Recipient's Catalog No.
NASA TN D-6397		

4. Title and Subtitle	5. Report Date
STATIC AERODYNAMIC CHARACTERISTICS OF A SCOUT FIN WITH AN ENLARGED TIP CONTROL AT MACH NUMBERS FROM 0.40 TO 4.63	September 1971
	6. Performing Organization Code
7. Author(s) Robert J. Keynton (Langley Research Center) and Thomas G. Muir (Missiles and Space Division, LTV Aerospace Corporation)	8. Performing Organization Report No. L-7680
	10. Work Unit No. 490-03-00-16
9. Performing Organization Name and Address NASA Langley Research Center Hampton, Va. 23365	11. Contract or Grant No.
	13. Type of Report and Period Covered Technical Note
12. Sponsoring Agency Name and Address National Aeronautics and Space Administration Washington, D.C. 20546	14. Sponsoring Agency Code

15. Supplementary Notes

16. Abstract

Results are presented of an experimental investigation to determine the static longitudinal aerodynamic characteristics of a fin with an enlarged tip control and the hinge-moment coefficients of the enlarged tip control. The model was tested at angles of attack from -6° to 6° and fin tip control deflections from -20° to 20°. A 1/8-scale model of the Scout first stage, with a tangent ogive nose, was used for these tests. Basic data obtained include the pitching-moment, rolling-moment, and normal-force coefficients of the fin and the hinge-moment coefficient of the enlarged tip control.

17. Key Words (Suggested by Author(s))	18. Distribution Statement
Aerodynamics Fin Fin tip control Static stability and control Scout	Unclassified – Unlimited

19. Security Classif. (of this report)	20. Security Classif. (of this page)	21. No. of Pages	22. Price*
Unclassified	Unclassified	52	$3.00

*For sale by the National Technical Information Service, Springfield, Virginia 22151

STATIC AERODYNAMIC CHARACTERISTICS OF A SCOUT FIN WITH AN ENLARGED TIP CONTROL AT MACH NUMBERS FROM 0.40 TO 4.63

By Robert J. Keynton
Langley Research Center

and

Thomas G. Muir
Missiles and Space Division
LTV Aerospace Corporation

SUMMARY

An experimental investigation has been conducted to determine the static longitudinal aerodynamic characteristics of a fin with an enlarged tip control and the hinge-moment coefficients of the enlarged tip control. Data were obtained at Mach numbers from 0.40 to 4.63 for an angle-of-attack range from -6° to 6° and fin tip control deflections from -20° to 20°. A 1/8-scale model of the Scout first stage, with a tangent ogive nose, was used for this investigation.

The results indicated linear stability and control characteristics of the fin. Maximum hinge-moment coefficients for the enlarged fin tip control occurred at Mach numbers of 0.40 and 0.59 and were essentially zero at a Mach number of 1.63 and higher Mach numbers. Results of limited testing at a Mach number of 1.00 indicated no significant effect of roll orientation.

INTRODUCTION

Increased use of the Scout launch vehicle as the workhorse of the aerospace research has created a demand for heavier and greater payload volume. To meet this demand the Scout Project Office embarked on the following two programs:

(1) Development of a larger first-stage motor

(2) Development of a larger heat shield

The economics of these developments influenced the configurations to the extent that the new motor and heat shield were to interface with existing transition sections or attach points. To achieve this objective, the new motor was increased in diameter with a conical frustum being placed at the fore and aft ends of the motor to interface with the

existing transition sections. Dynamic stability studies showed that the existing aerodynamic control surfaces did not produce sufficient control authority. The obvious solution was to increase the surface area of the tip control. The location of the aft frustum is very close to the stabilizing fins and, therefore, it is very difficult to evaluate the flow in the vicinity of the fin with accuracy or confidence. Since the Scout vehicle has a marginal static margin at maximum dynamic pressure ($M \approx 3.00$), it was mandatory to acquire sufficient data to define with confidence the aerodynamic characteristics of the proposed configuration.

The purpose of this investigation was to determine experimentally the fin longitudinal stability and control characteristics in order to define the stability margins for the new Scout configuration. A limited discussion is presented of the test results.

SYMBOLS

The aerodynamic coefficients are referred to the body-axis system illustrated in figure 1. The moment reference center was 14.526 cm (5.719 in.) from the cylindrical base. The hinge line was located at two-thirds of the mean aerodynamic chord of the fin tip, 1.32 cm (0.521 in.) from the tip trailing edge. The data are given in both SI and U.S. Customary Units. The measurements and calculations were made in U.S. Customary Units.

A reference-body cross-sectional area, 0.0076078 meter^2 (0.08189 foot^2)

b exposed span of two fins with two enlarged fin tips, 24.78 centimeters (0.813 foot)

C_h hinge-moment coefficient, $\frac{\text{Hinge moment}}{qSc}$

C_l rolling-moment coefficient, $\frac{\text{Rolling moment}}{qAd}$

C_{l_δ} rate of change of rolling-moment coefficient with fin tip control deflection, $\frac{\partial C_l}{\partial \delta}$, per degree

C_m pitching-moment coefficient, $\frac{\text{Pitching moment}}{qAd}$

C_{m_α} slope of pitching-moment curve at $\alpha = 0^o$, $\frac{\partial C_m}{\partial \alpha}$, per degree

C_{m_δ} rate of change of pitching-moment coefficient with fin tip control deflection at $\alpha = 0^o$, $\frac{\partial C_m}{\partial \delta}$, per degree

C_N normal-force coefficient, $\frac{\text{Normal force}}{qA}$

C_{N_α} slope of normal-force curve at $\alpha = 0^o$, $\frac{\partial C_N}{\partial \alpha}$, per degree

C_{N_δ} rate of change of normal-force coefficient with fin tip control deflection at $\alpha = 0^o$, $\frac{\partial C_N}{\partial \delta}$, per degree

c average geometric chord of fin tip control, 0.019571 meter (0.064208 foot)

c_r exposed root chord of fin, 11.430 centimeters (0.375 foot)

c_r' root chord of enlarged fin tip control, 3.967 centimeters (0.130 foot)

d reference diameter, 0.09842 meter (0.3229 foot)

M free-stream Mach number

q free-stream dynamic pressure, newtons/meter^2 (pounds/foot^2)

S fin tip control planform area, 0.000786778 meter^2 (0.0084688 foot^2)

x_{cp} distance aft of leading edge along root chord to center of pressure, centimeters (feet)

y_{cp} spanwise distance from body surface to center of pressure, centimeters (feet)

α angle of attack of fin plane of symmetry, degrees

β sideslip angle (nose down is $+\beta$), for $\phi = 90^o$, degrees

δ fin tip control deflection, positive to provide nose-down pitching moment at $\phi = 0^o$ (leading edge up), degrees

ϕ roll angle, measured between instrumented fin plane of symmetry and horizontal reference plane, positive for clockwise roll as viewed looking forward, degrees

APPARATUS AND TESTS

Test Facilities

This investigation was conducted at two test facilities. The transonic test section of the Vought Aeronautics Company High Speed Wind Tunnel was utilized for testing from M = 0.40 to 1.63. This facility is a blowdown-to-atmosphere, transonic-supersonic, adjustable Mach number installation. The nozzle upstream from the test section is an adjustable contour type and consists of two flexible stainless-steel plates and two fixed walls. The test section is 1.22 m (4 ft) square. A more detailed description of this facility is presented in reference 1.

The low and high Mach number test sections of the Langley Unitary Plan wind tunnel were utilized for testing from M = 1.90 to 4.63. This tunnel is a variable-pressure, continuous-flow facility. The nozzle upstream from the test section is the asymmetric sliding-block type which permits a Mach number variation from 1.50 to 2.86 in the low Mach number test section and from 2.30 to 4.63 in the high Mach number test section. The sliding-block arrangement also permits the test-section length and cross-sectional area to remain relatively constant (2.13 m (7 ft) and 1.49 m^2 (16 ft^2), respectively) throughout the Mach number range.

Model

Details of the 1/8-scale model are presented in figure 2. The model consisted of the Scout first stage (Algol-III) with a tangent ogive nose and simulated wiring tunnels. One fin was mounted on a six-component internal strain-gage balance which measured the forces and moments on the exposed fin. Of those six components, only normal force, pitching moment, and rolling moment are presented herein. These components are used to define magnitude and location of the fin lift and center of pressure for simulating the vehicle flight with a computer program. Fin deflection or rotation due to air loads was not evaluated. This fin contained an enlarged tip control mounted on an instrumented shaft. The shaft, and consequently the fin tip, was rotated between tests. The deflection angles were set by means of a locating pin (fig. 2(c)) and a set of precisely located holes at the base of the fin. After the deflection angle was set, the shaft—fin-tip combination was locked in place by two set screws located in the root of the fin. The locating pin was then removed and the test was resumed. The fin area and tip area were determined by previous wind-tunnel tests and theoretical studies (refs. 2 to 5). The other three fins were attached directly to the body and had the standard Scout fin configuration. For Mach numbers up to and including 1.9, a transition strip of No. 60 carborundum grit embedded in a plastic adhesive 0.16 cm (1/16 in.) wide was applied around the nose 3.05 cm (1.20 in.) aft of the nose apex (measured on the surface) for the purpose of insuring a

turbulent boundary layer downstream. Similar transition strips were applied to the fins and fin tip control 1.016 cm (0.40 in.) aft (streamwise) of the leading edge. For Mach numbers above 1.9, a transition strip of No. 45 carborundum grit embedded in a plastic adhesive, one granule wide, was applied to the nose at the same location as for the lower Mach numbers. The transition strips on the instrumented fin and fin tip control were also of No. 45 carborundum grit and were applied at the same locations as for the lower Mach numbers. The size and location of the carborundum grit are selected as predicted by the unique flow conditions of the individual facility.

Tests

The experimental data were obtained at Mach numbers from 0.40 to 4.63 for an angle-of-attack range from -6° to 6°. Six-component fin force and moment data and fin tip control hinge-moment data were obtained for fin tip control deflections from 10° to -20° at Mach numbers up to and including 1.63 and from 20° to -20° at Mach numbers above 1.63. The model was tested primarily with the instrumented fin in the horizontal plane ($\phi = 0^{\circ}$) and selected tests were made for $\phi = 45^{\circ}$ and 90° at $M = 1.00$. Test conditions are presented in table I.

Measurements

Complete model aerodynamic forces and moments were measured by a six-component internal strain-gage balance. This balance was mounted on a sting which was part of the model support system. The data from this balance were used to evaluate sting deflections due to aerodynamic loads. Actual fin aerodynamic forces and moments, as noted previously, were measured by the fin balance. Hinge-moment gages were installed on the mounting shaft of the enlarged fin tip control. The axis system used is shown in figure 1. When observing that figure, it is important to remember that the fin normal force remains normal to the plane containing the fin and model longitudinal center line. Consequently, when the model is rolled, both the fin and the normal-force vector rotate through the same angle ϕ.

Corrections

Model angle of attack was corrected for tunnel airflow misalinement and deflection of the sting and sting-mounted balance due to aerodynamic loads.

RESULTS AND DISCUSSION

The static longitudinal stability and control characteristics of the model fin are presented in figure 3. The variations of fin C_N and C_m with α and δ are linear

except at combined high angles of attack and fin tip control deflection at Mach numbers below 0.60. Except at the higher supersonic Mach numbers, the fin tips appear to stall at these high values of α and δ. The longitudinal stability characteristics are summarized in figure 4. Correlation of data obtained from the various test facilities is excellent. The longitudinal control effectiveness for one fin tip control is summarized in figure 5.

Fin rolling-moment-coefficient data are presented in figure 6; the variation of C_l with angle of attack is linear except at combined high angles of attack and fin tip control deflection. The roll control effectiveness for one fin tip control is summarized in figure 7. Hinge-moment-coefficient data for the enlarged fin tip control are presented in figure 8. Maximum hinge-moment coefficients occur at $M = 0.40$ and 0.59; thereafter, the hinge-moment coefficient decreases as Mach number increases up to $M = 1.63$. At $M = 1.63$ and higher, the coefficient is essentially zero and is relatively invariant at combined high angles of attack and fin tip control deflection.

Figures 9 to 11 present fin data at $M = 1.00$ for $\phi = 0^\circ$ and 45° and $\delta = 0^\circ$ and -10°. With $\phi = 45^\circ$, the instrumented fin is on the windward side of the body at positive angles of attack. In figure 9, the data show that as the instrumented fin is rotated to the leeward side of the body, the increment in fin force resulting from either α or δ is reduced. This reduction is attributed to decreased flow angularity and dynamic pressure on the leeward side of the body. This decrease is not indicated on the windward side between $\phi = 0^\circ$ and 45°.

Figures 12 to 14 present fin data at $M = 1.00$ for $\phi = 0^\circ$ and 90° and $\delta = -10^\circ$. The $\delta = 0^\circ$ data were omitted at $\phi = 90^\circ$ because the instrumented fin is moving in the vertical plane and, consequently, the measured forces are zero. For $\phi = 90^\circ$, the model was pitched in the same wind-tunnel plane as for $\phi = 0^\circ$ and 45°; thus, the variable model attitude angle was sideslip angle β instead of angle of attack α. At $\alpha = \beta = 0^\circ$, the forces and moments on the fin are the same for both roll angles with $\delta = -10^\circ$ because the model flow fields are equivalent. The increment in fin force due to a -10° fin tip control deflection is less at $\alpha = -6^\circ$ than it is at $\alpha = 6^\circ$. (See fig. 12.)

CONCLUDING REMARKS

Results of an investigation to determine the static longitudinal aerodynamic characteristics (pitching-moment, rolling-moment, and normal-force coefficients) of a Scout fin and the hinge-moment coefficients of the enlarged fin tip control indicate that the coefficients are predominately linear throughout the test ranges of Mach number ($M = 0.40$ to 4.63) and angle of attack ($\alpha = -6^\circ$ to 6°). Below and including $M = 1.90$, the pitching-moment, rolling-moment, and normal-force coefficients are linear for $\alpha = -4^\circ$ to 4°. Above and including $M = 2.30$, these coefficients are linear for $\alpha = -6^\circ$ to 6°. The

hinge-moment coefficient C_h is extremely nonlinear through $M = 1.39$. Above that Mach number, C_h not only is linear but is effectively nonexisting.

At low Mach numbers and high angles of attack and tip control deflection, the data indicate that the fin tip control has a tendency to stall. Above $M = 1.00$ the tendency to stall at combined high angles of attack and tip control deflection continued, but Mach number ceased to be an influencing parameter.

Langley Research Center,
National Aeronautics and Space Administration,
Hampton, Va., August 24, 1971.

REFERENCES

1. Arnold, John W.: High Speed Wind Tunnel Facility Handbook. Publ. No. AER-EIR-13552-B, Vought Aeronautics Co., Feb. 1970. (Revised Mar. 1971.)

2. Scout Eng.: Study of Effects of Incorporating a Larger Heatshield on the Scout Vehicle. Rep. No. 23.411 (Contract No. NAS1-6935), Missiles & Space Div., LTV Aerosp. Corp., July 24, 1969. (Available as NASA CR-111947.)

3. Keynton, Robert J.: Longitudinal Stability Characteristics of Preliminary Configurations for Scout D at Mach Numbers 0.20 to 4.63. NASA TN D-6239, 1971.

4. Yanowitch, S.; and Knauber, R. N.: Scout First Stage Flight Characteristics. Rep. No. 23.358 (Contract No. NAS1-6020), Missiles & Space Div., LTV Aerosp. Corp., Mar. 15, 1968. (Available as NASA CR-111945.)

5. Brassard, J. A.; Knauber, R. N.; and Melugin, J. E.: Scout First Stage Moment Disturbance Study. Rep. No. 23.287 (Contract No. NAS1-4664-EDJ), LTV Astronaut. Div., July 15, 1966. (Available as NASA CR-111946.)

TABLE I.- TEST CONDITIONS

M	Dynamic pressure		Reynolds number	
	newtons/meter^2	pounds/foot^2	per meter	per foot
0.40	16 662	348	12.927×10^6	3.94×10^6
.59	33 085	691	17.520	5.34
.81	46 108	963	20.669	6.30
.90	50 131	1047	19.849	6.05
1.00	55 110	1151	20.341	6.20
1.10	59 324	1239	20.833	6.35
1.20	62 244	1300	19.455	5.93
1.39	66 123	1381	19.915	6.07
1.63	73 831	1542	22.507	6.86
1.90	34 426	719	9.843	3.00
2.30	32 606	681	↓	↓
2.96	27 627	577		
3.95	21 307	445		
4.63	16 758	350		

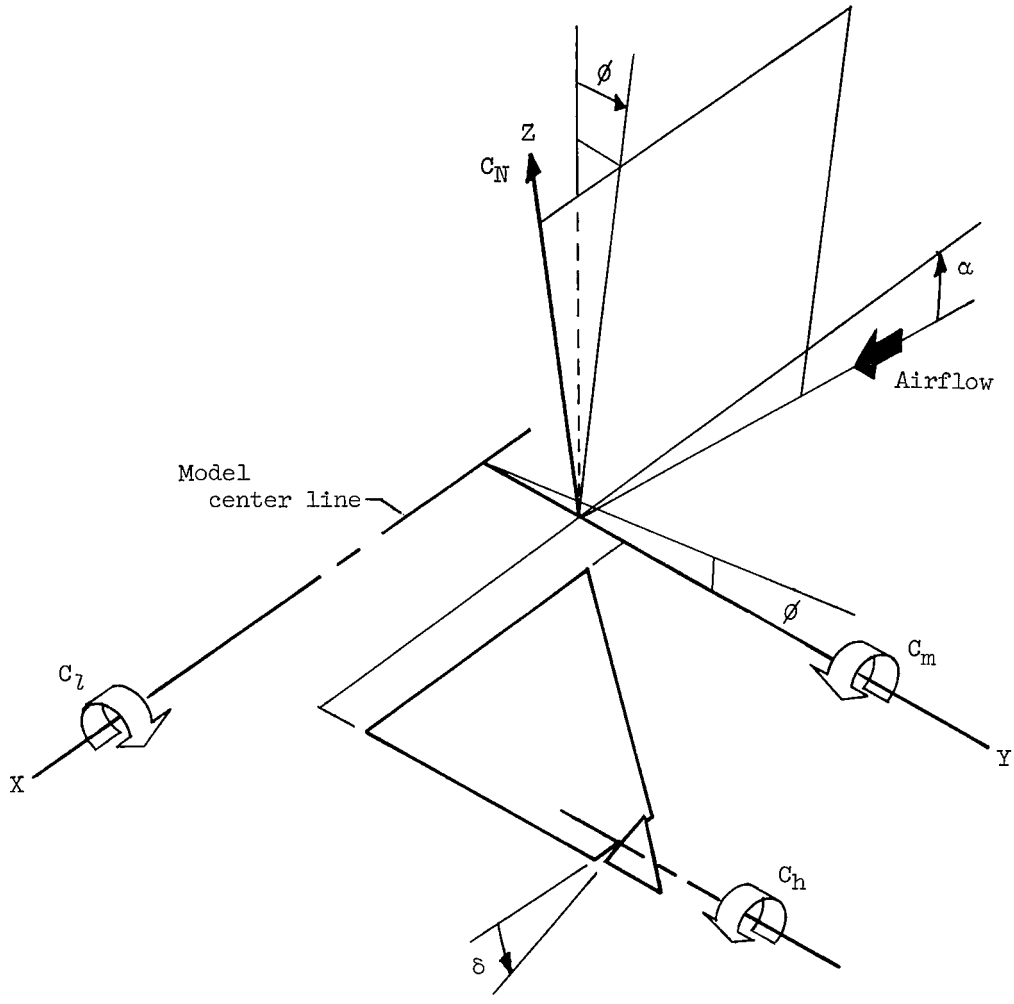

Figure 1.- Body-axis system. Arrows indicate positive direction.

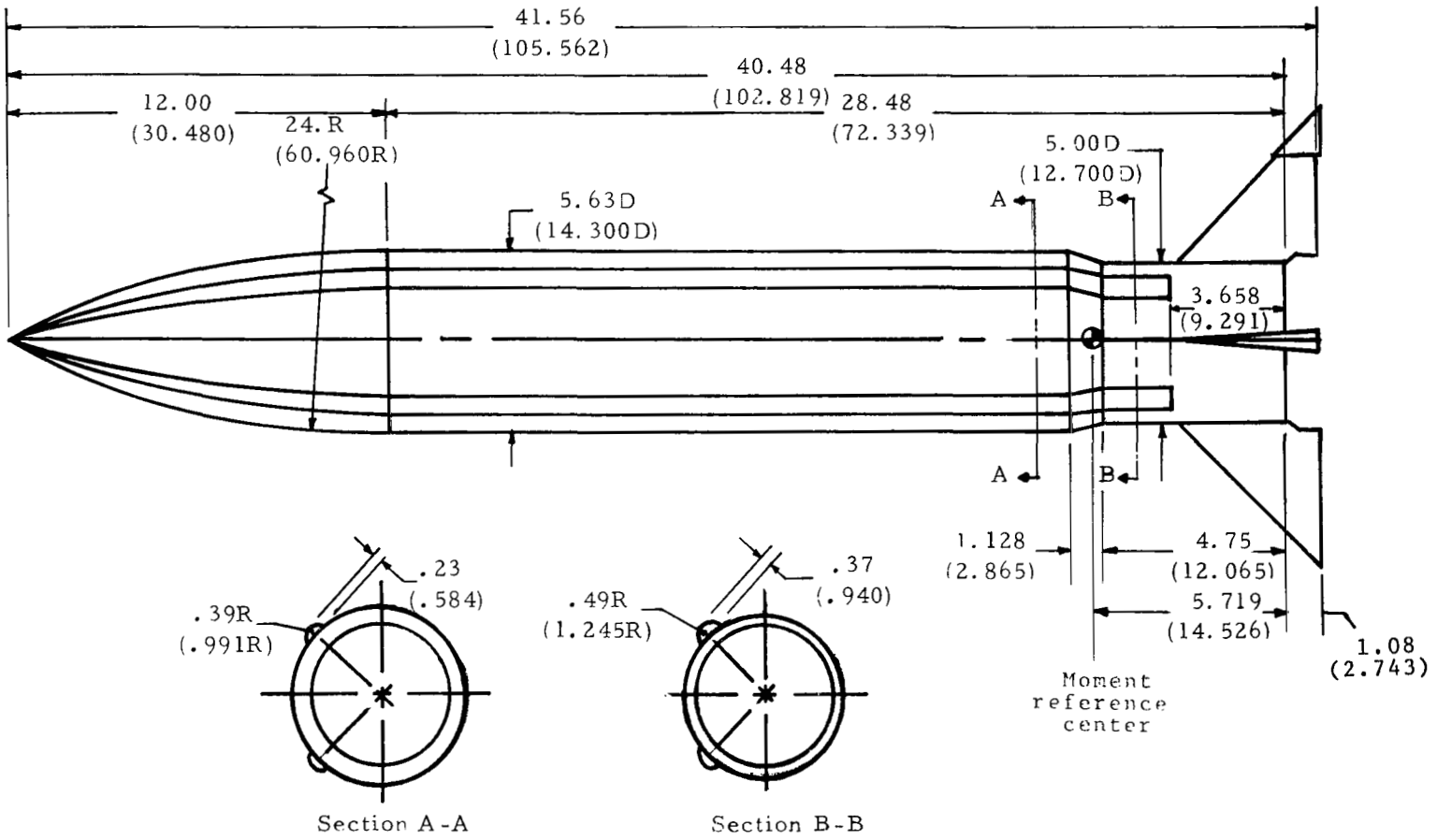

(a) Complete model.

Figure 2.- Model details. Dimensions are in inches (centimeters).

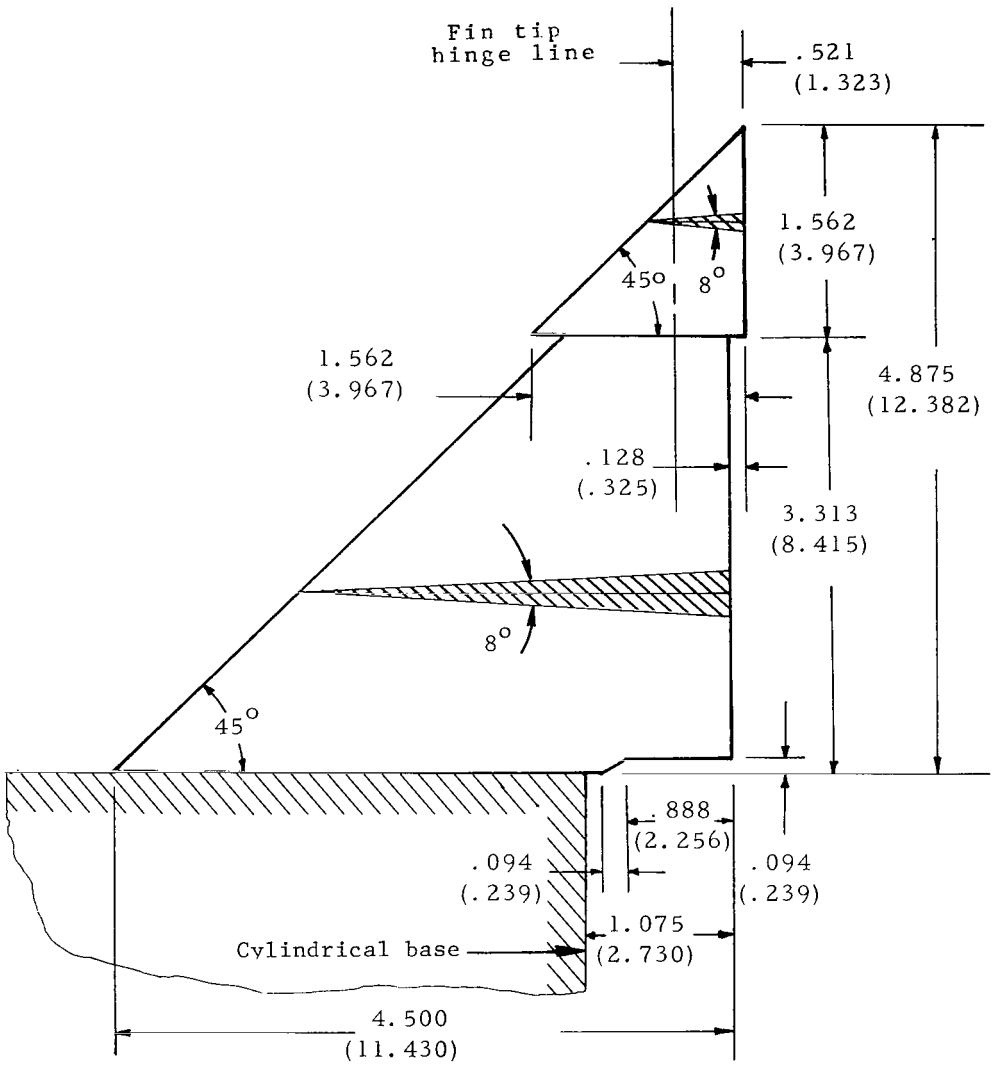

(b) Fin with enlarged fin tip control.

Figure 2.- Continued.

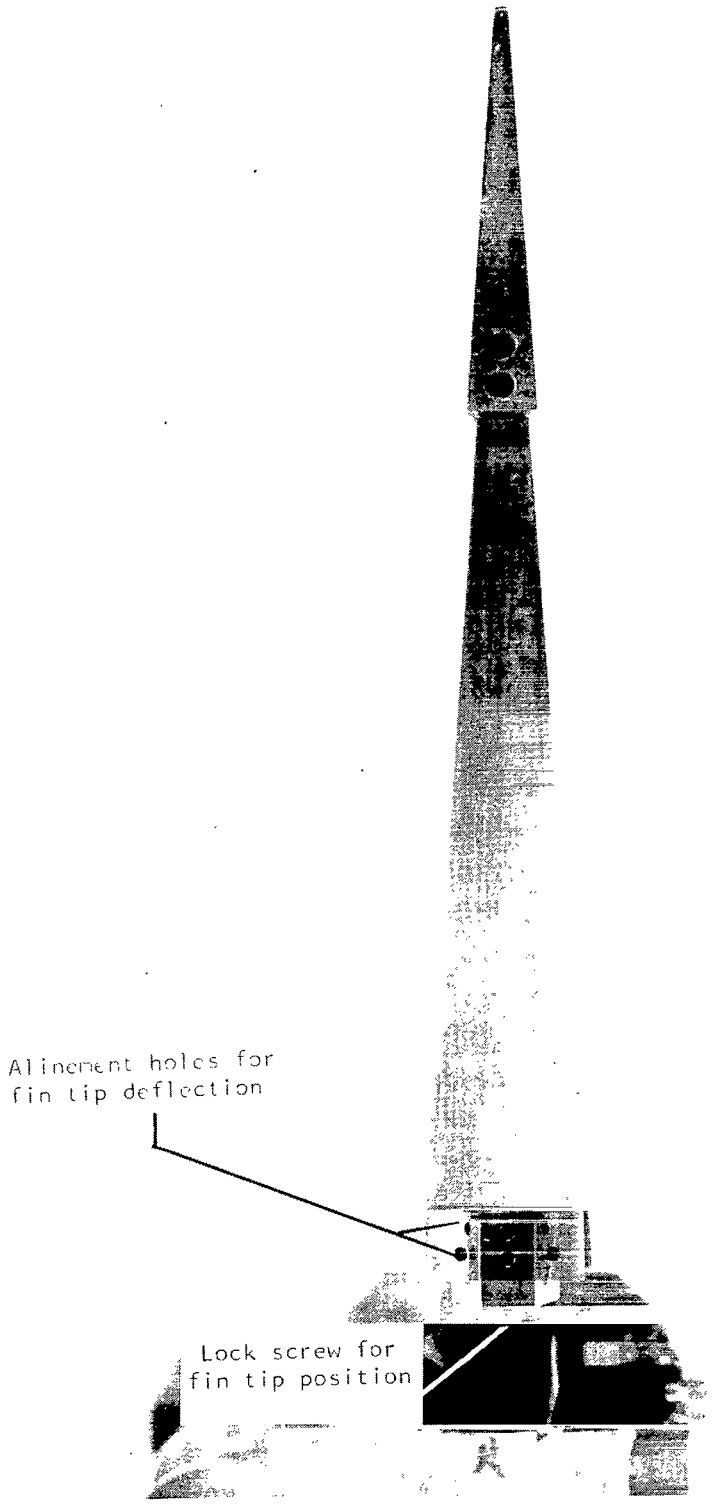

L-71-2755.1

(c) Instrumented fin trailing edge.

Figure 2.- Concluded.

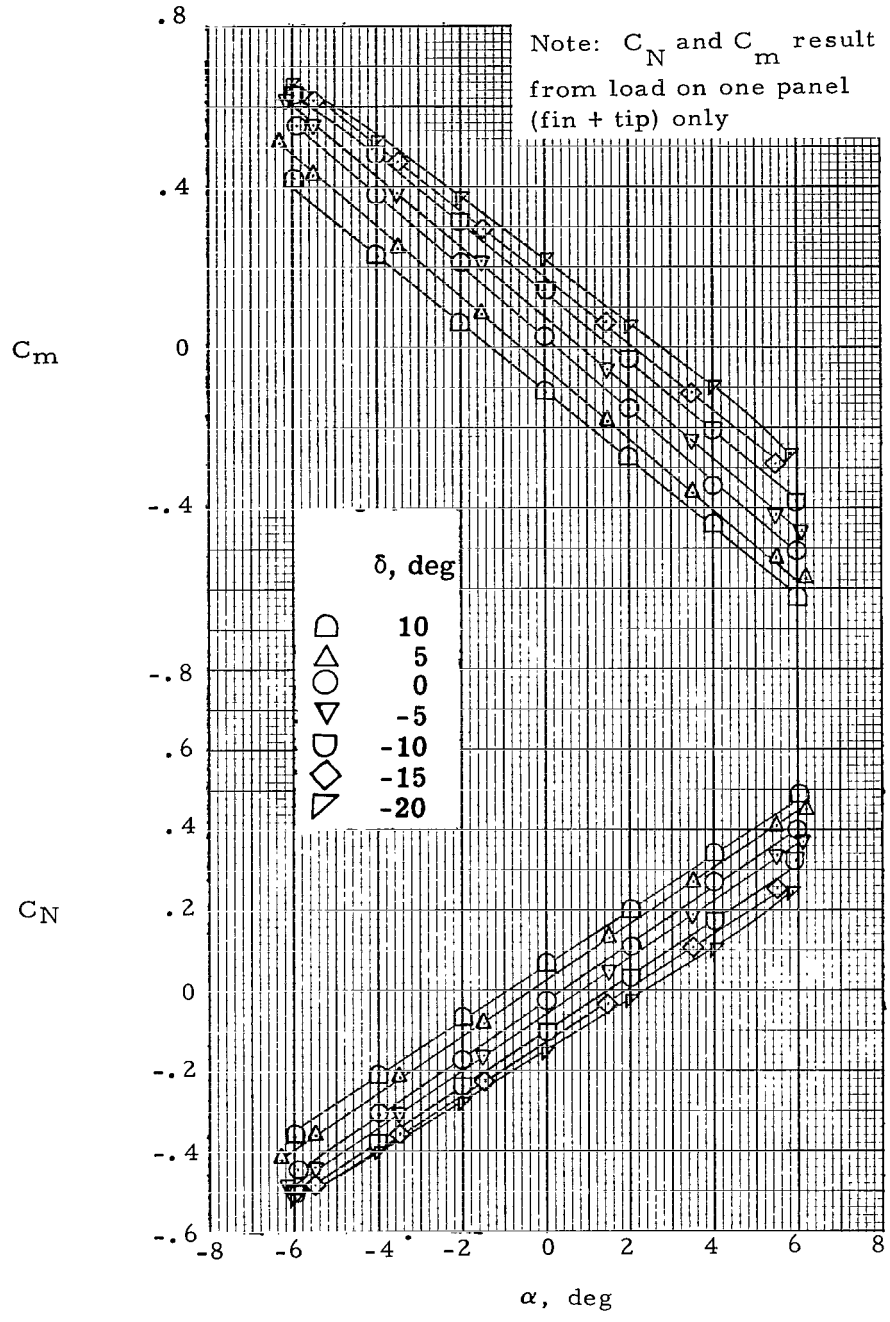

(a) M = 0.40.

Figure 3.- Static longitudinal stability and control characteristics of fin. $\phi = 0^{o}$.

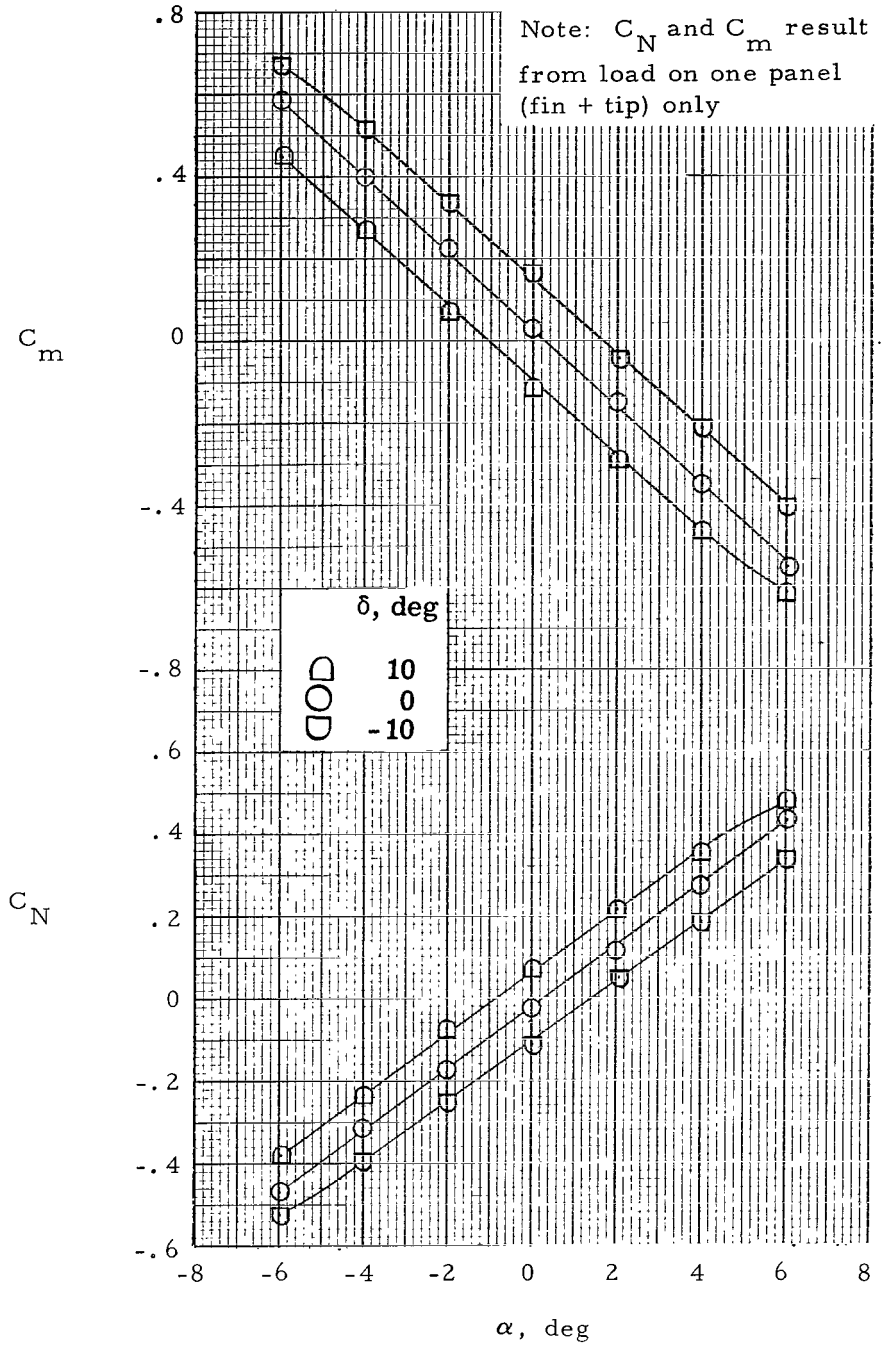

(b) M = 0.59.

Figure 3.- Continued.

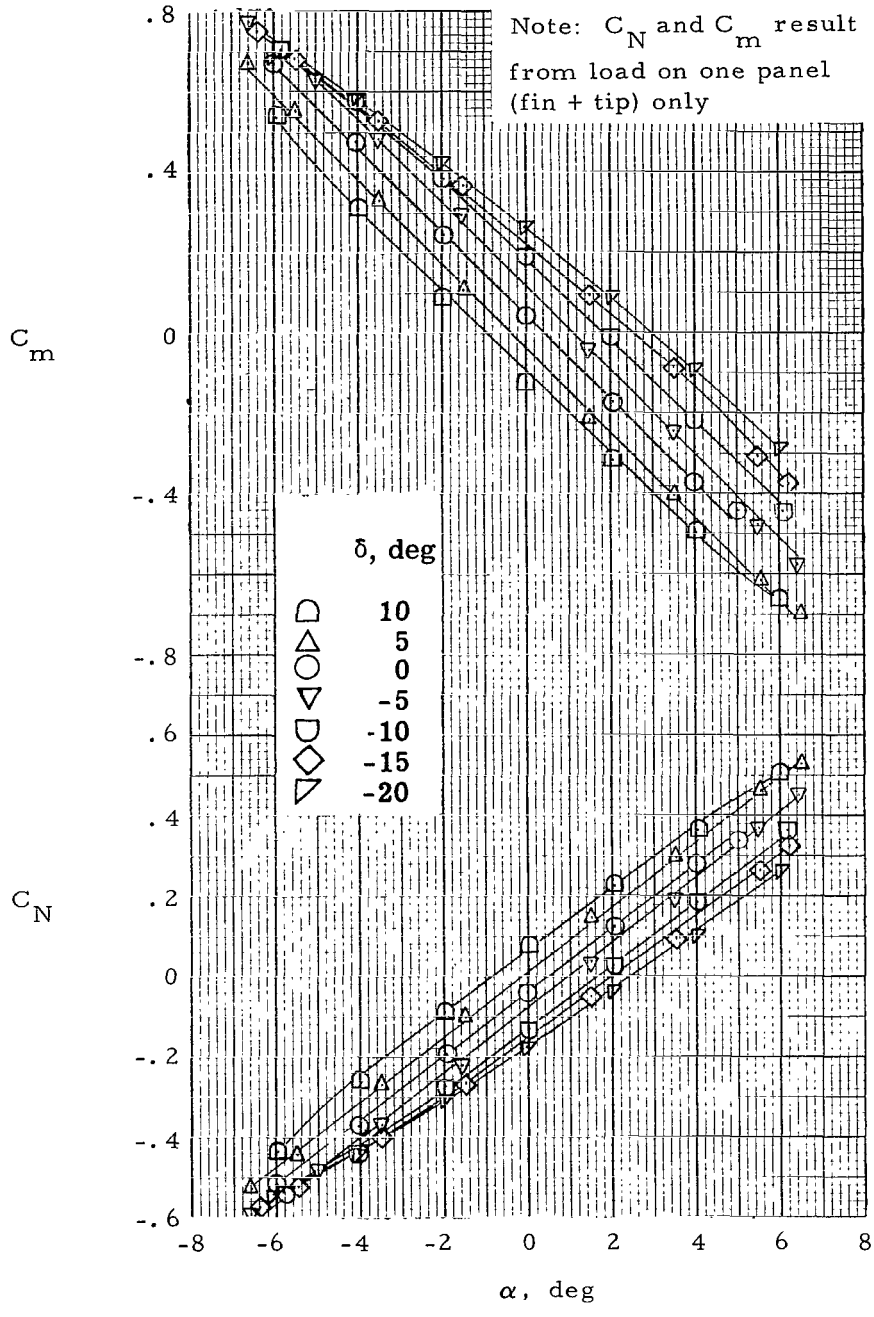

(c) M = 0.81.

Figure 3.- Continued.

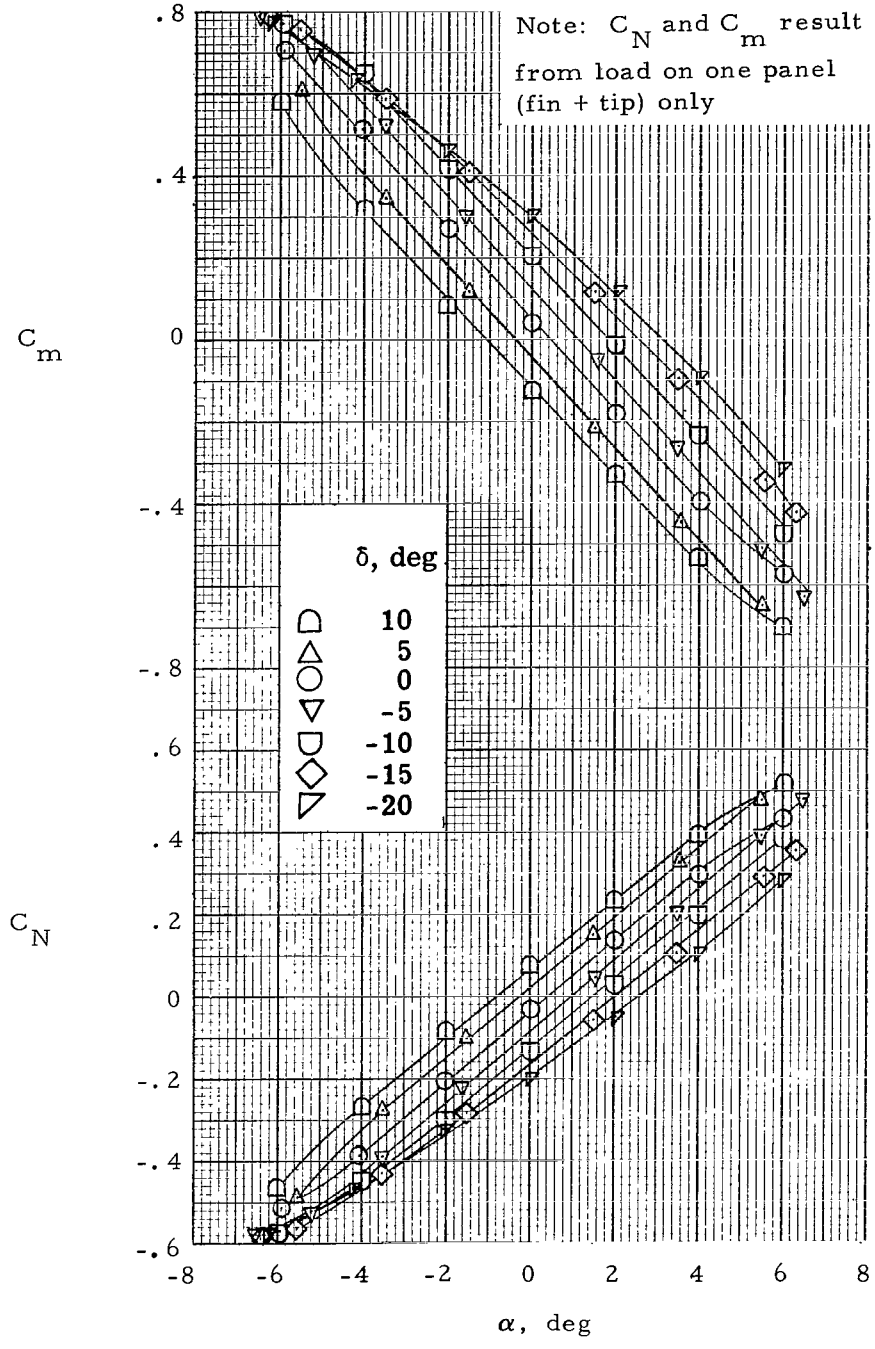

(d) M = 0.90.

Figure 3.- Continued.

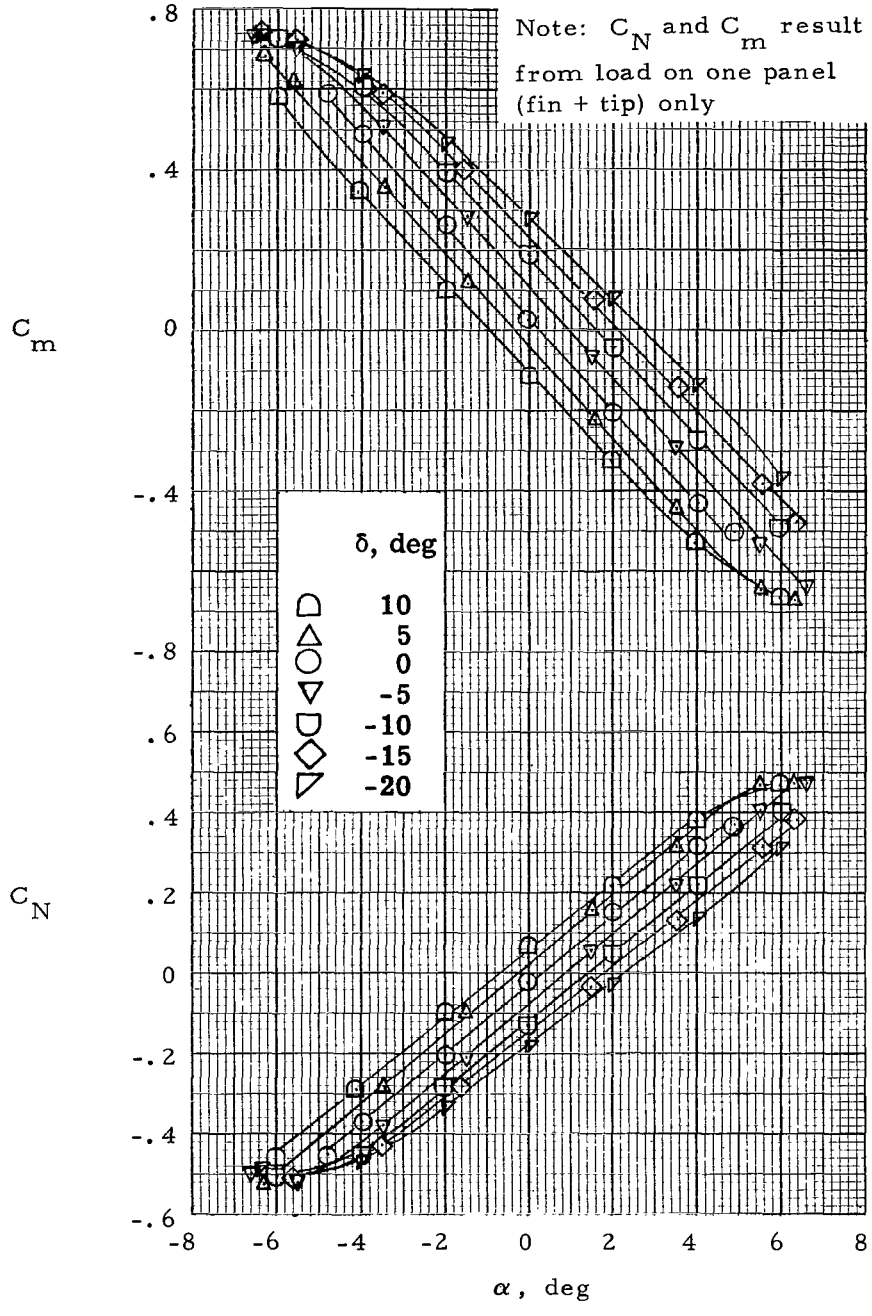

(e) M = 1.00.

Figure 3.- Continued.

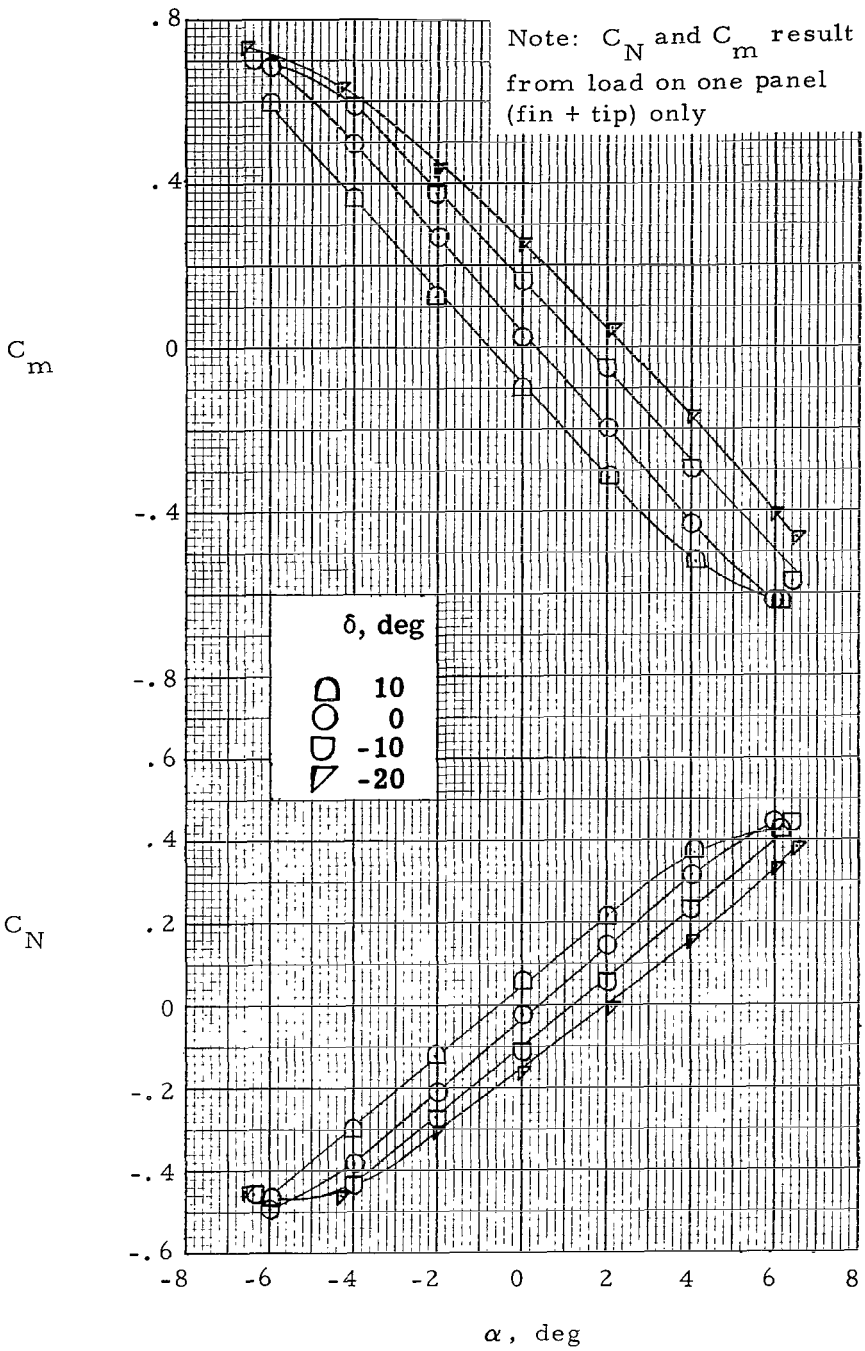

(f) M = 1.10.

Figure 3.- Continued.

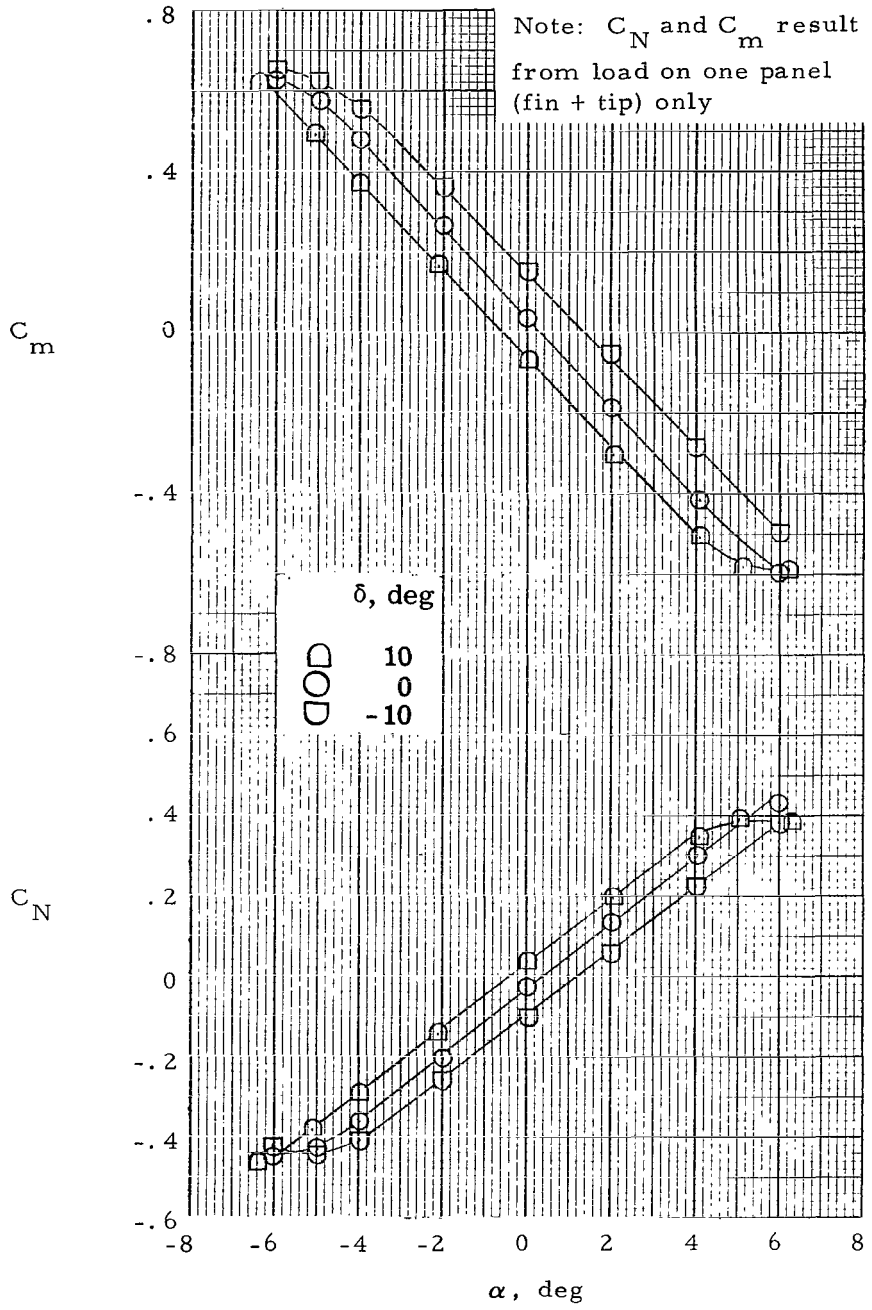

(g) M = 1.20.

Figure 3.- Continued.

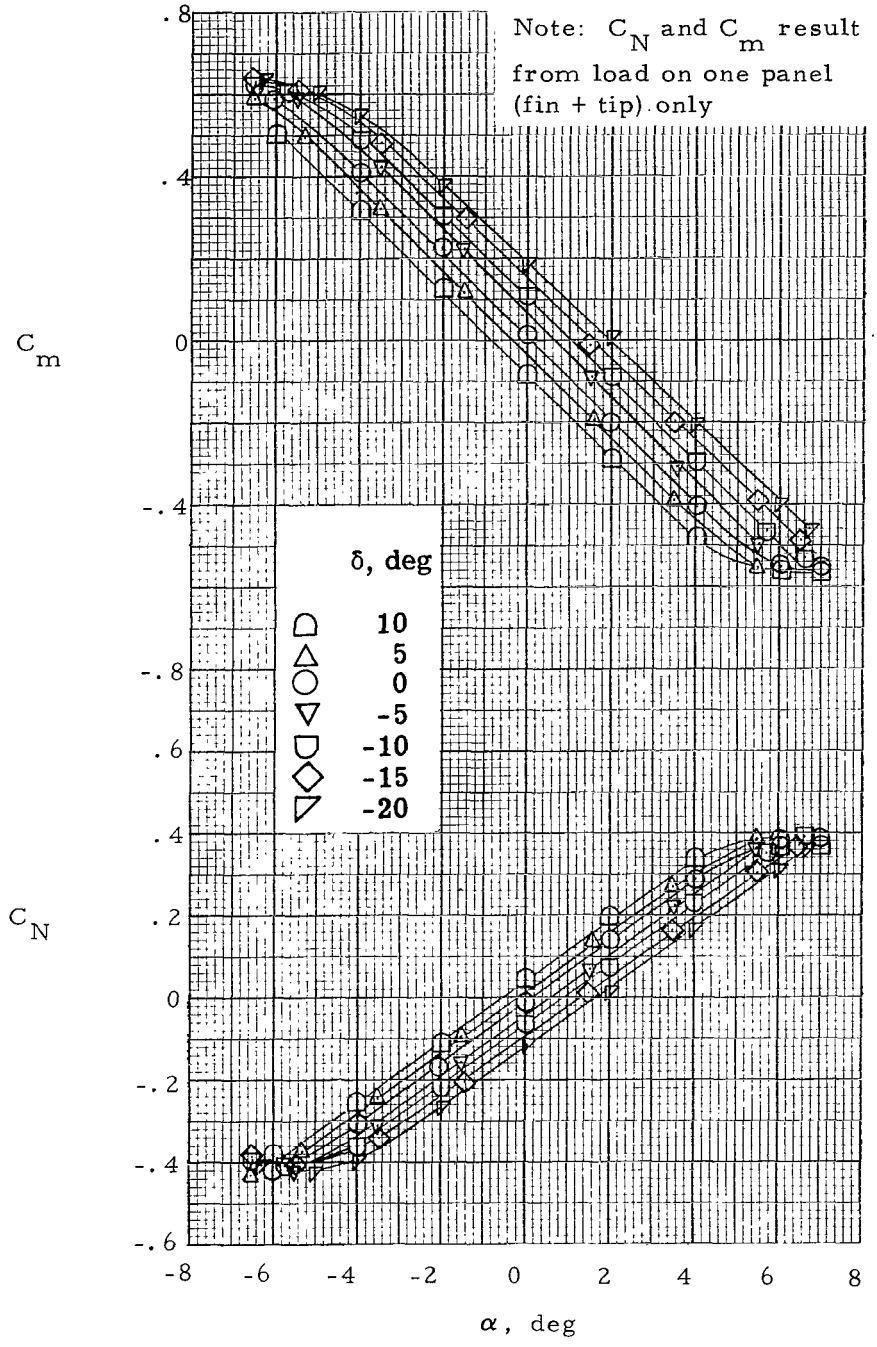

(h) M = 1.39.

Figure 3.- Continued.

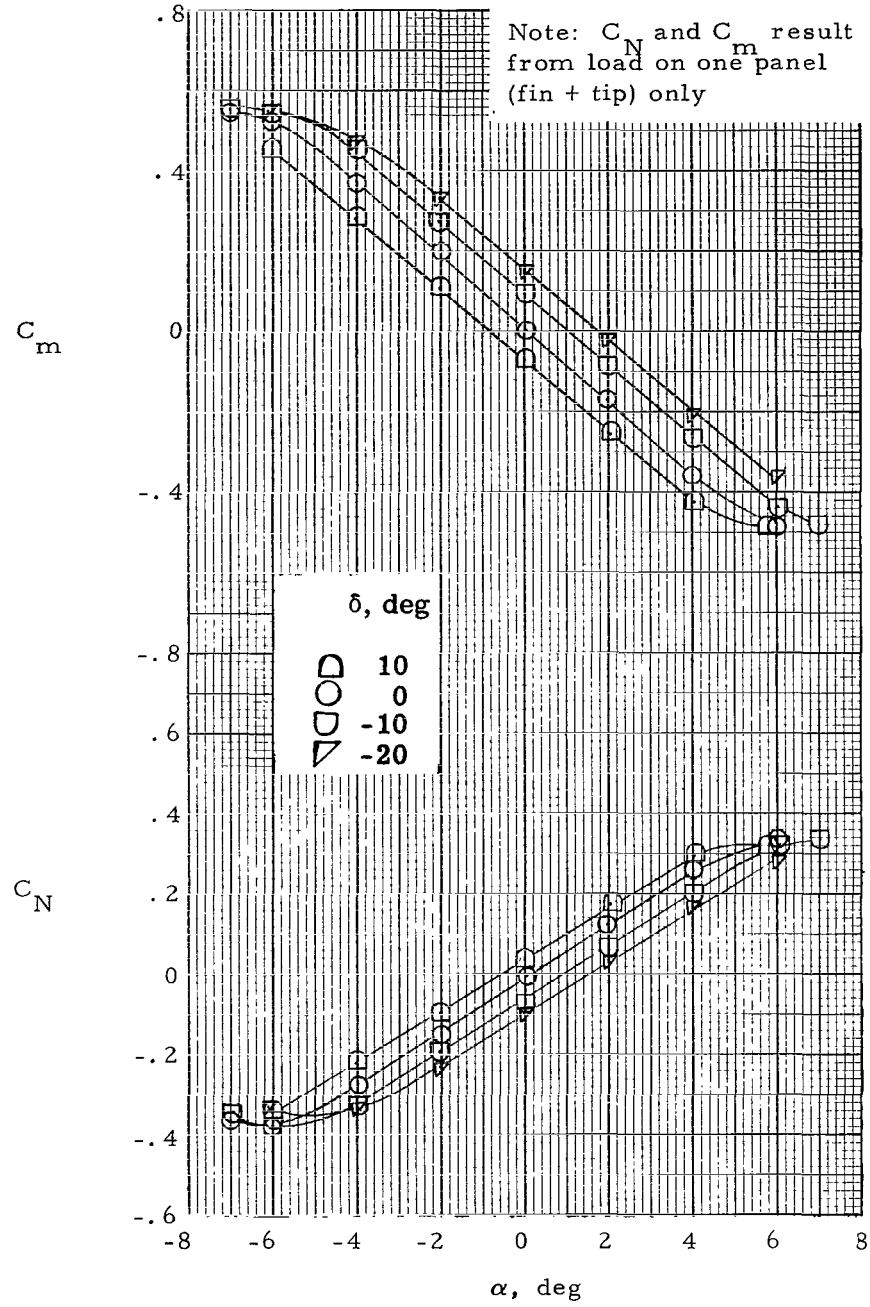

(i) M = 1.63.

Figure 3.- Continued.

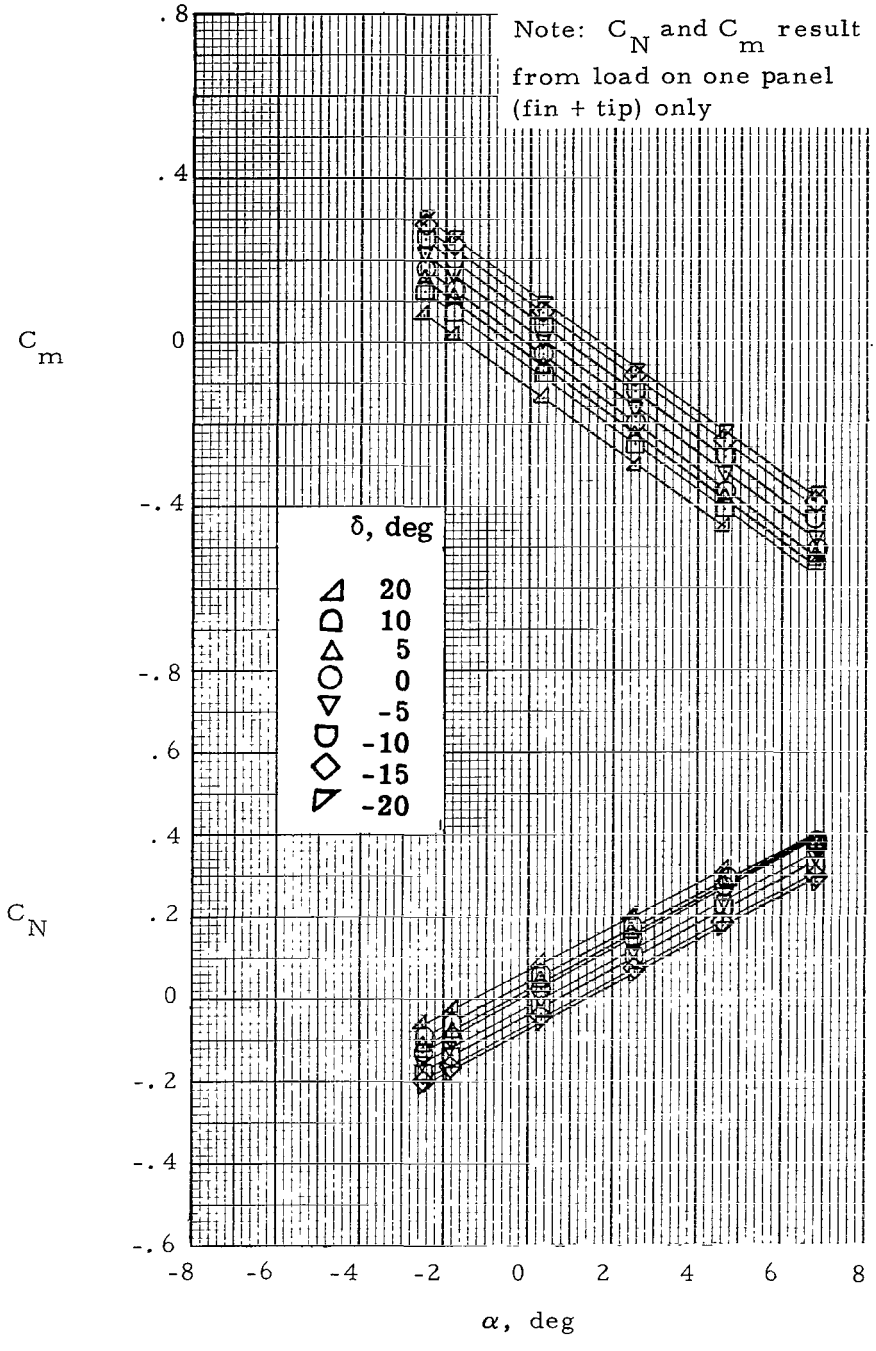

(j) M = 1.90.

Figure 3.- Continued.

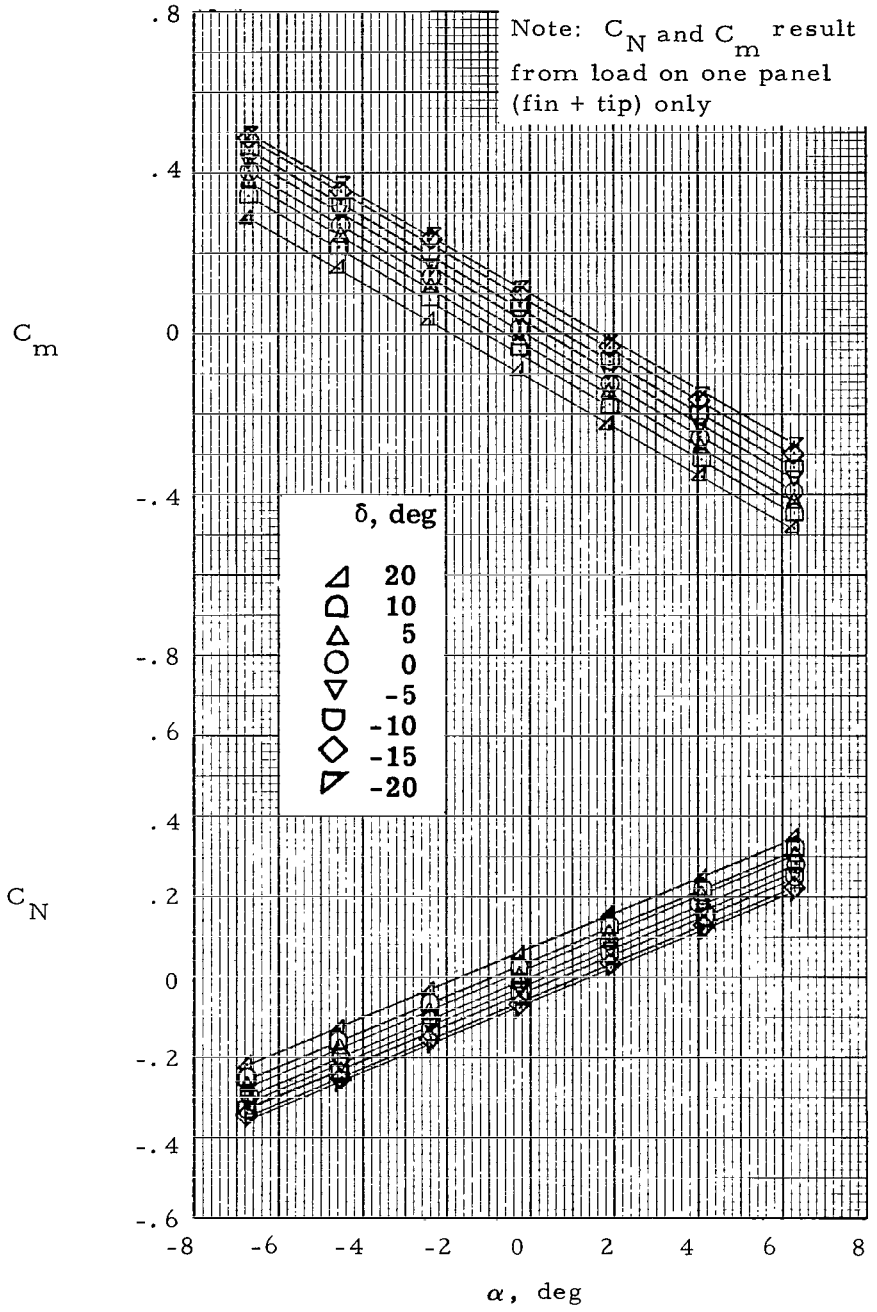

(k) M = 2.30.

Figure 3.- Continued.

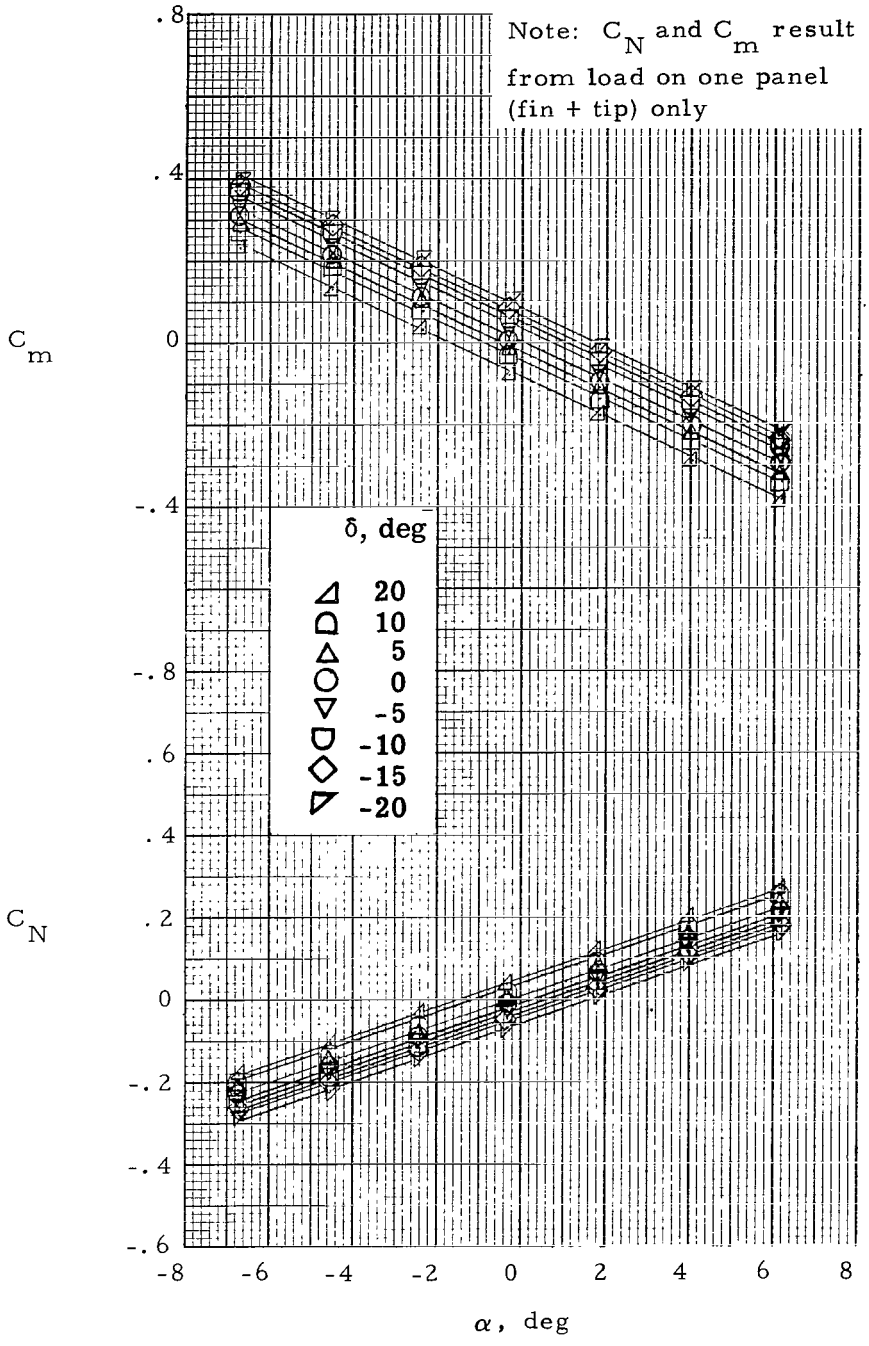

(l) M = 2.96.

Figure 3.- Continued.

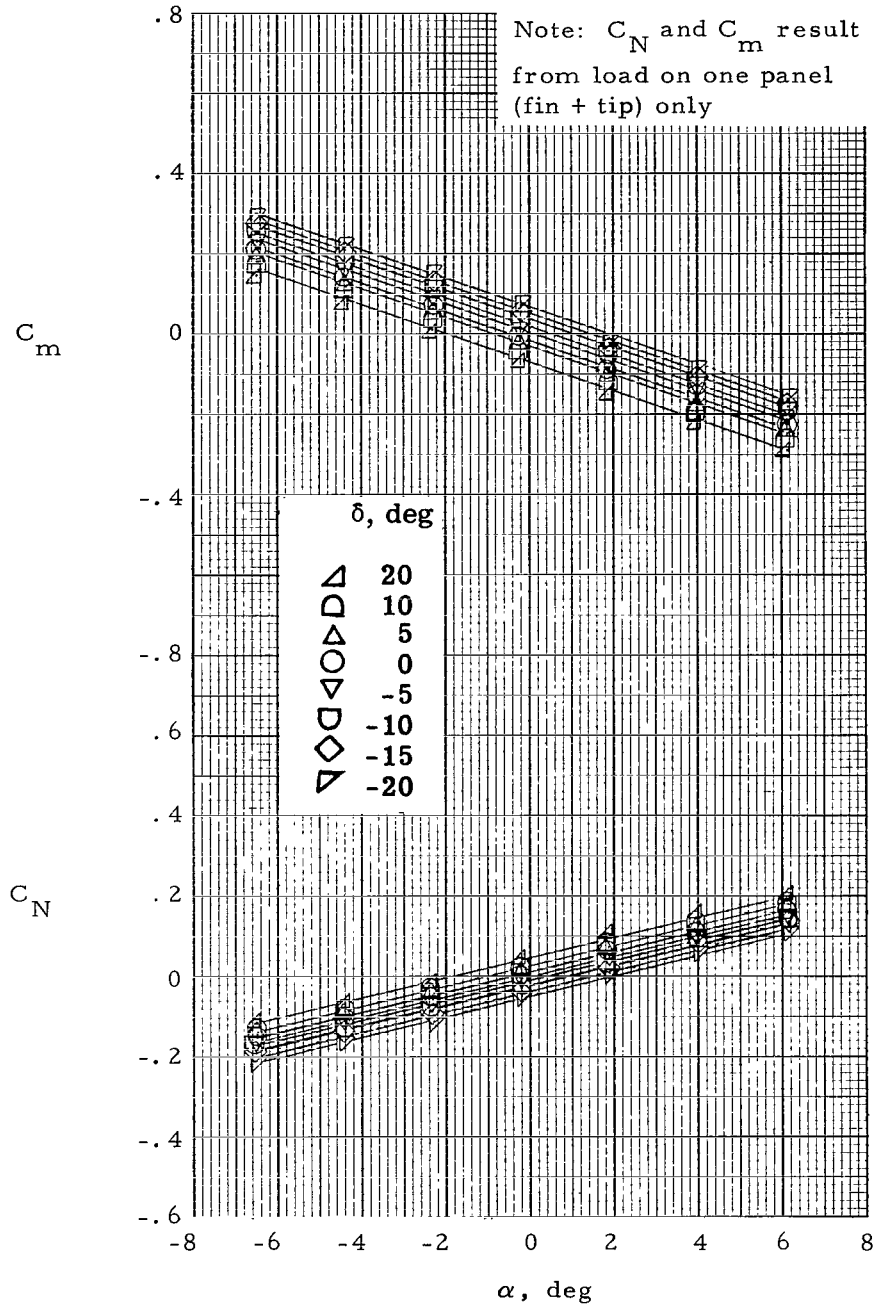

(m) M = 3.95.

Figure 3.- Continued.

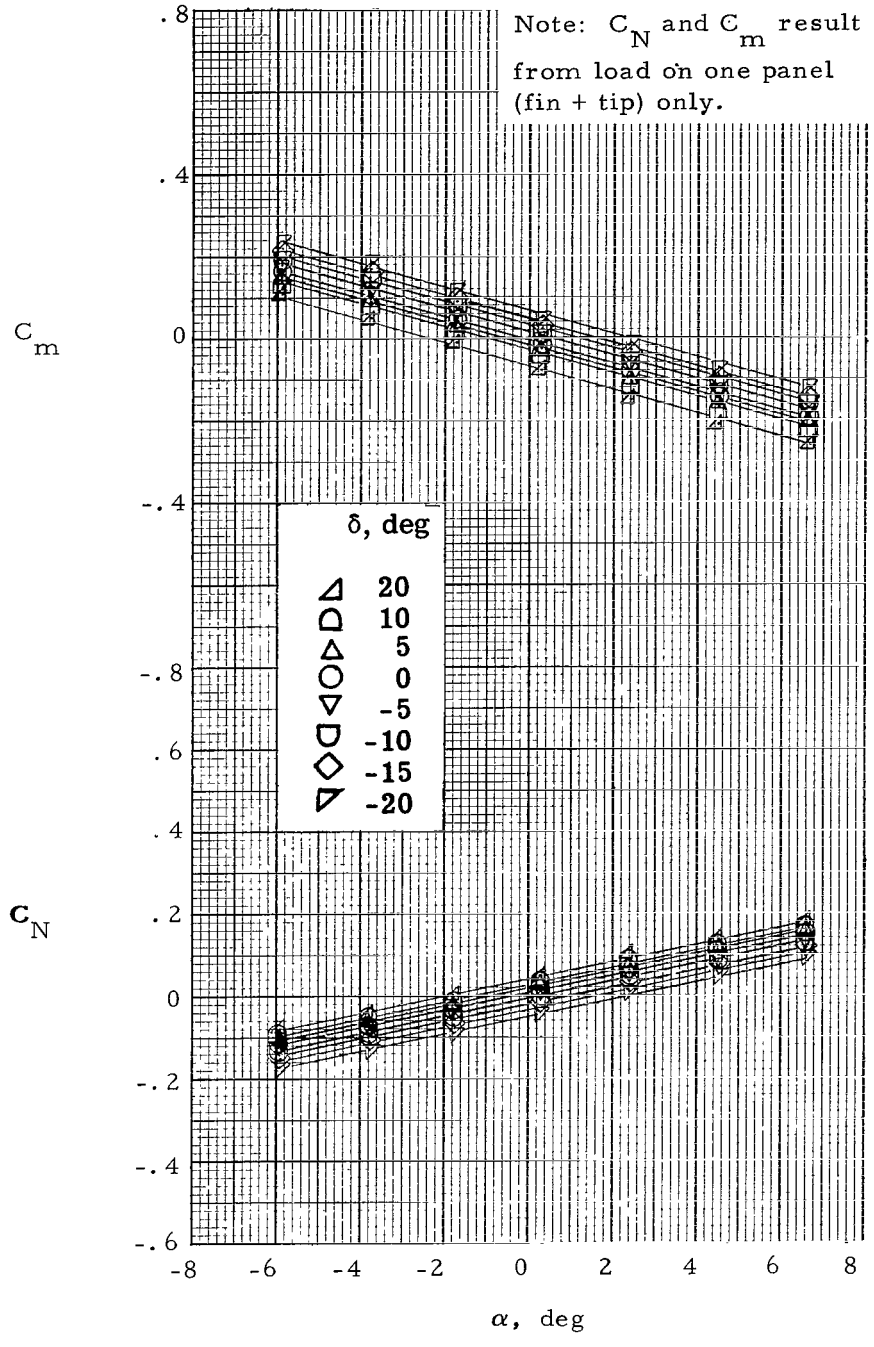

(n) M = 4.63.

Figure 3.- Concluded.

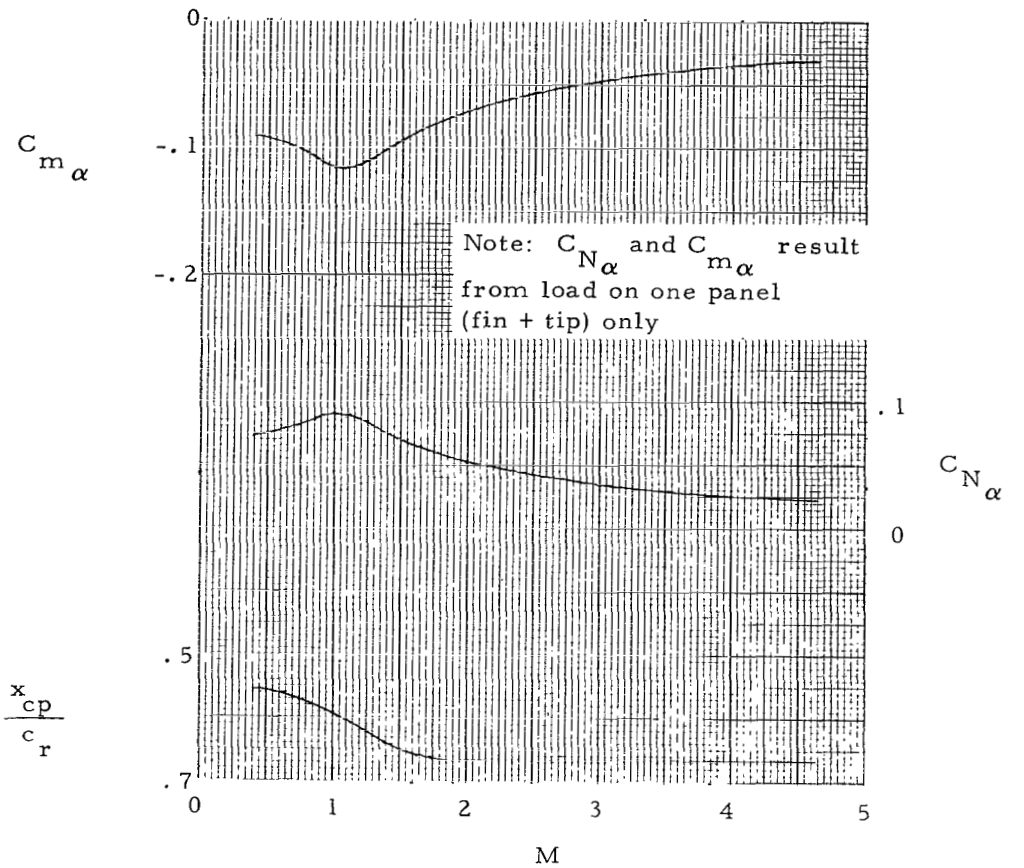

Figure 4.- Summary of longitudinal stability characteristics of fin.

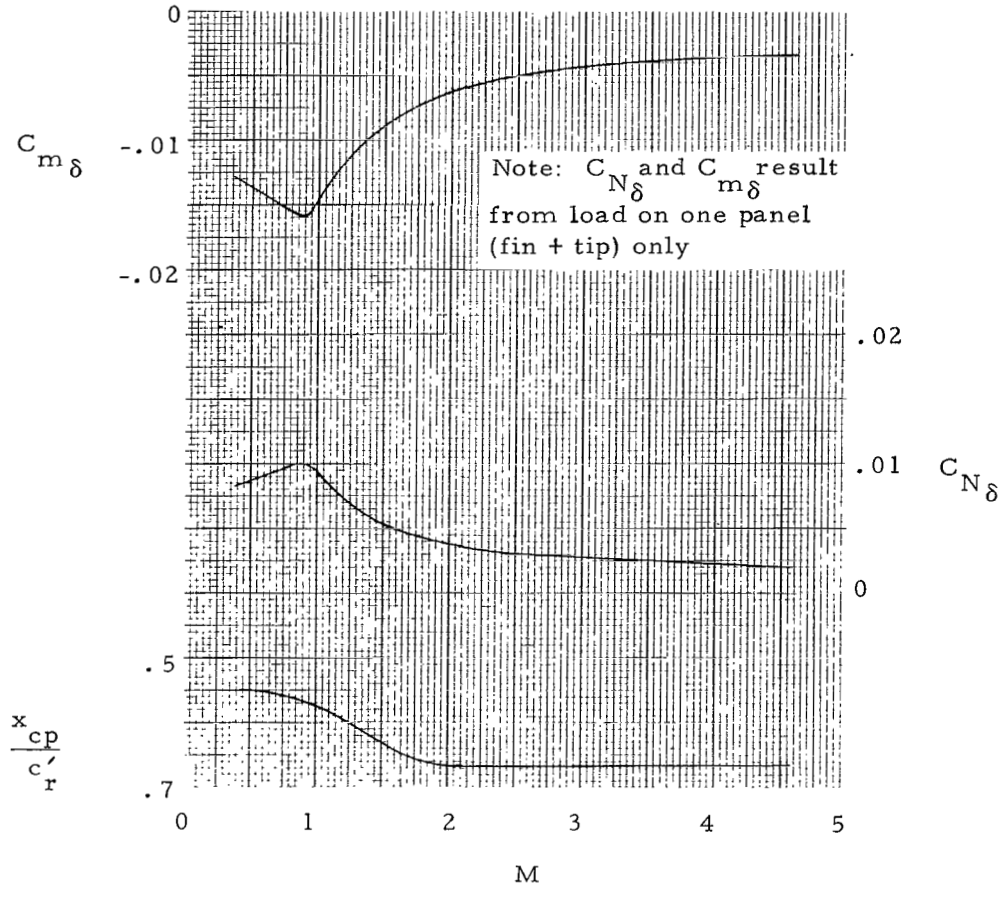

Figure 5.- Summary of longitudinal control effectiveness of one fin tip control.

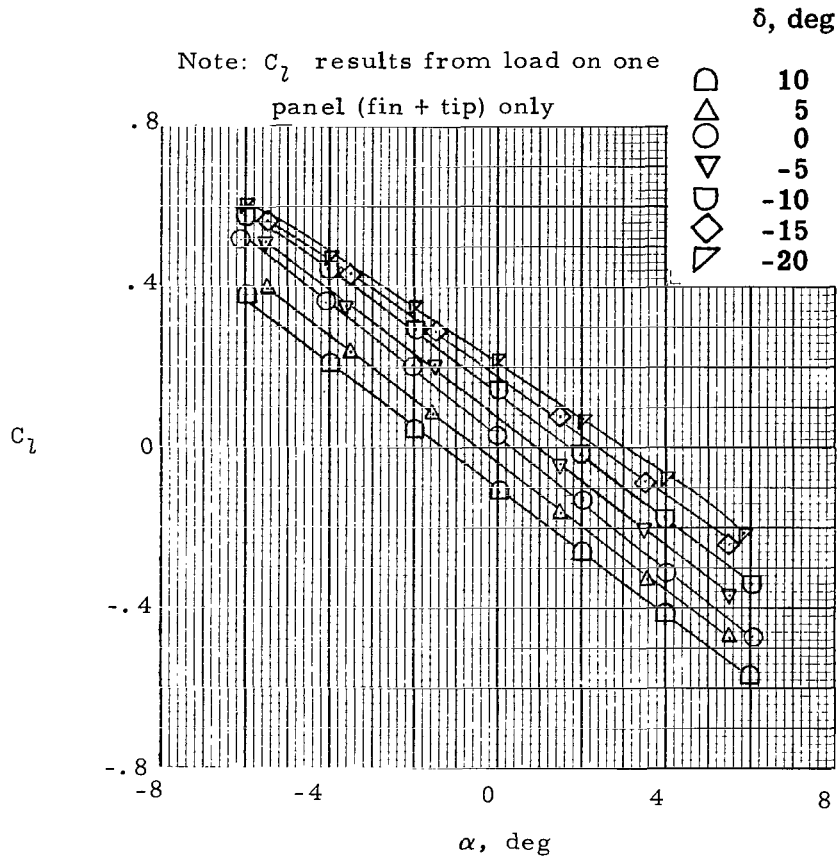

(a) M = 0.40.

Figure 6.- Fin rolling-moment coefficient. $\phi = 0^{o}$.

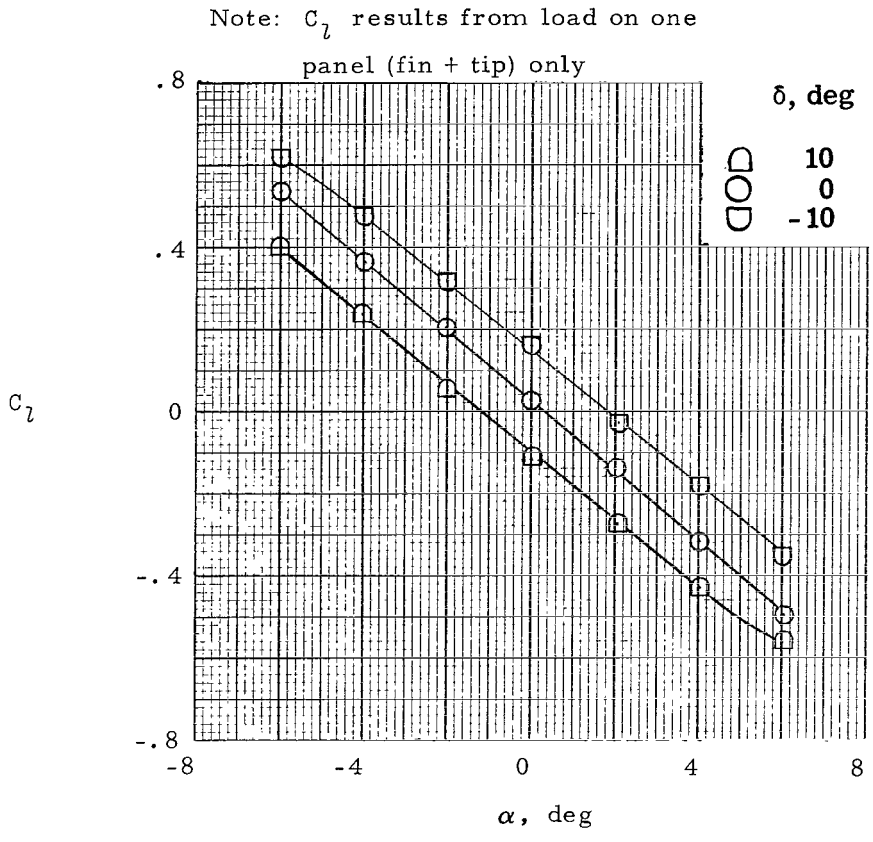

(b) M = 0.59.

Figure 6.- Continued.

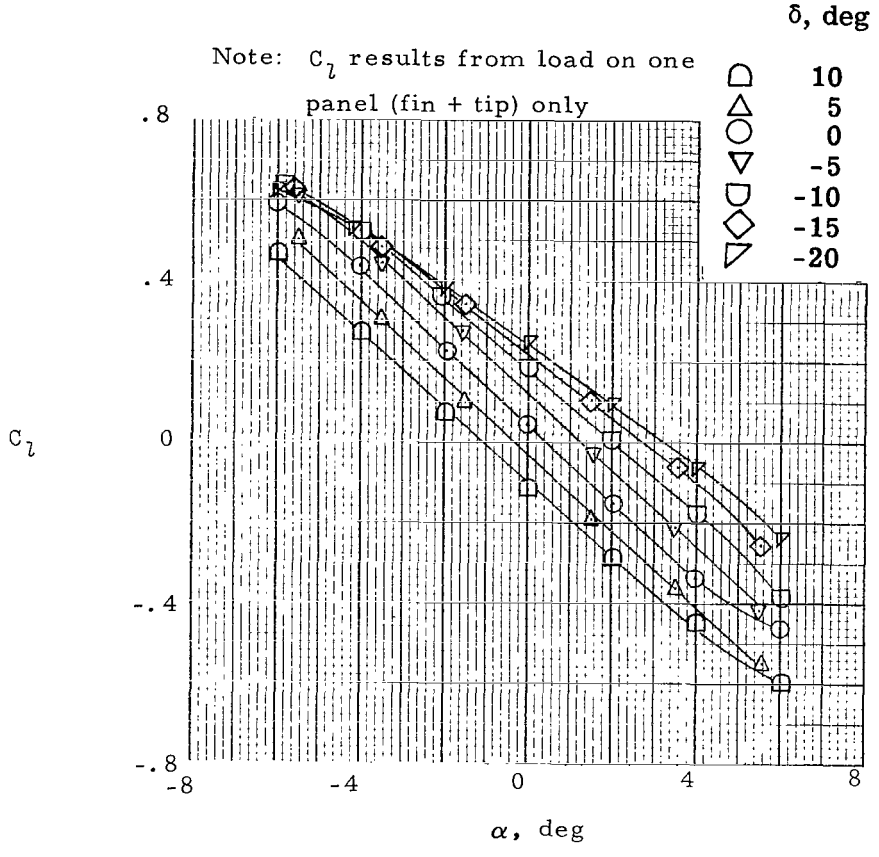

(c) M = 0.81.

Figure 6.- Continued.

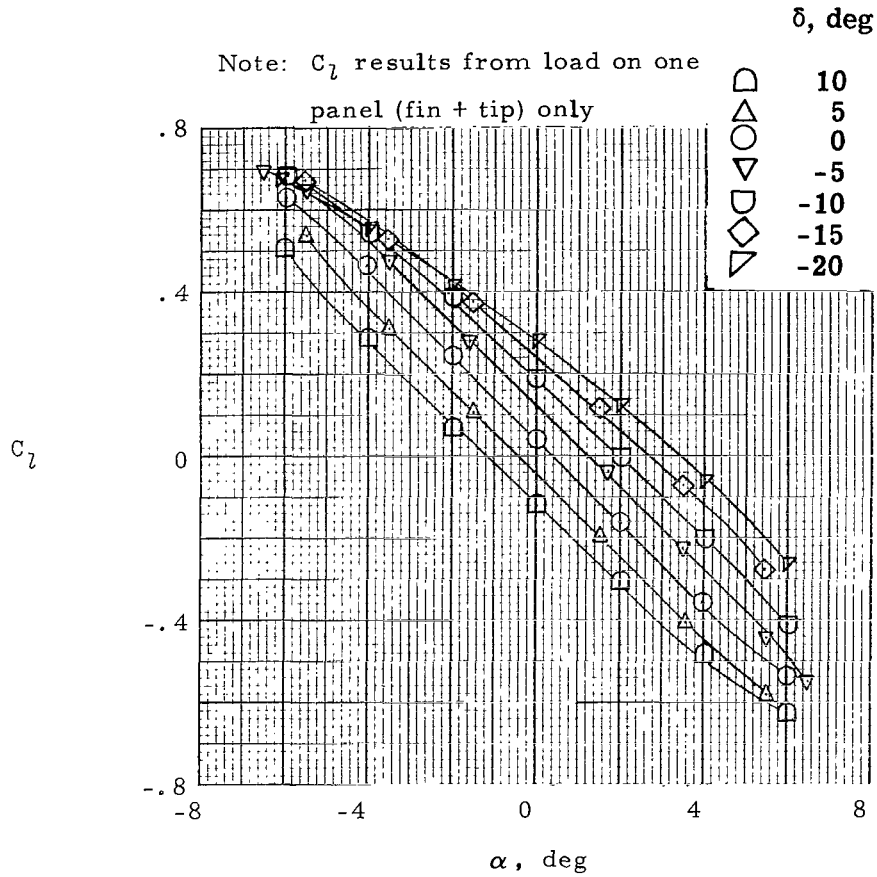

(d) M = 0.90.

Figure 6.- Continued.

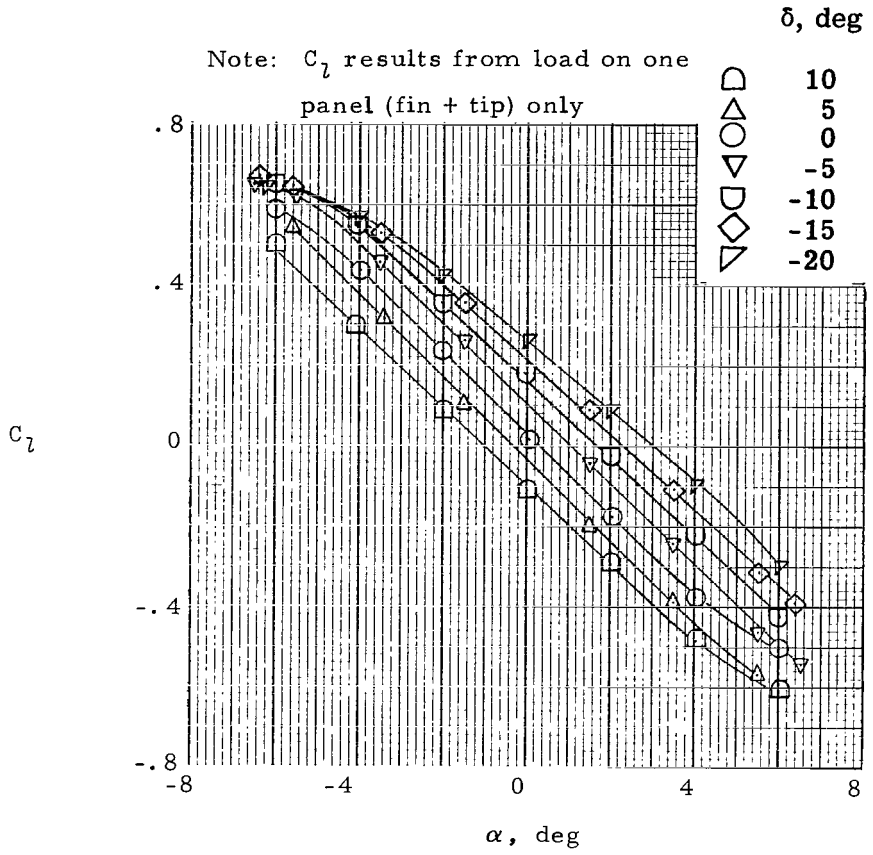

(e) M = 1.00.

Figure 6.- Continued.

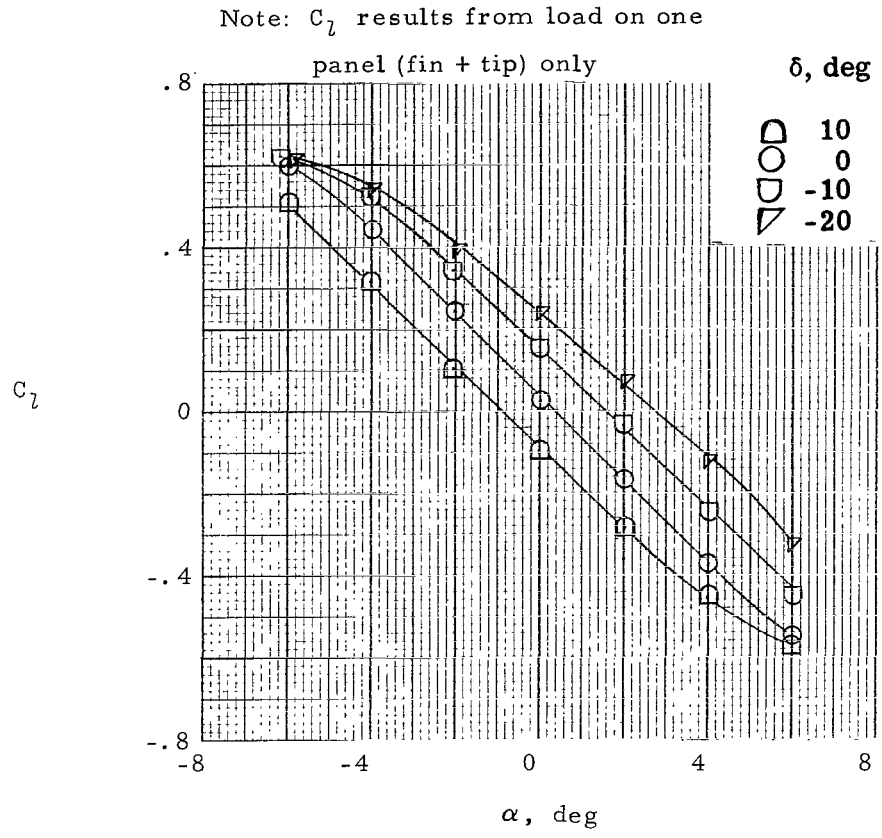

(f) M = 1.10.

Figure 6.- Continued.

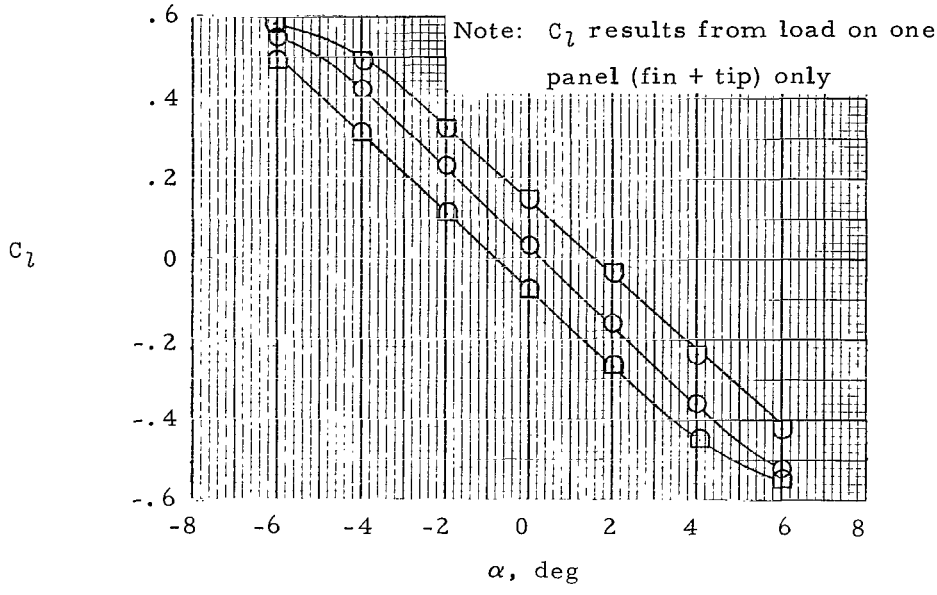

(g) M = 1.20.

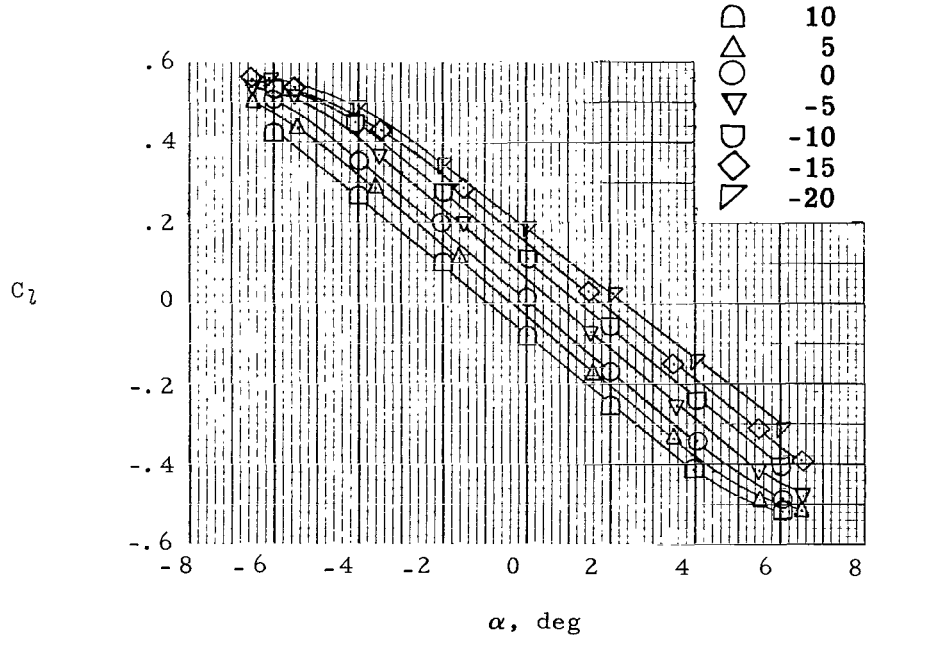

(h) M = 1.39.

Figure 6.- Continued.

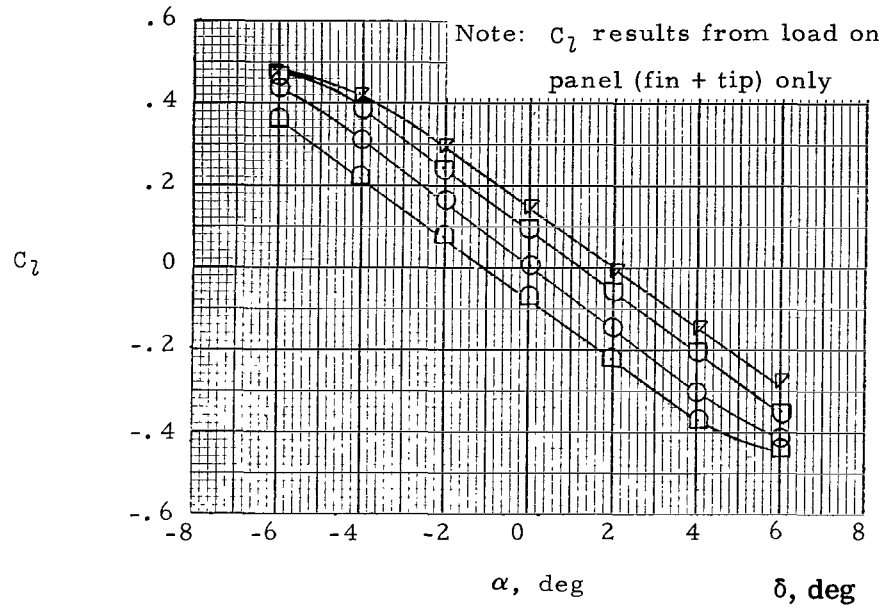

(i) M = 1.63.

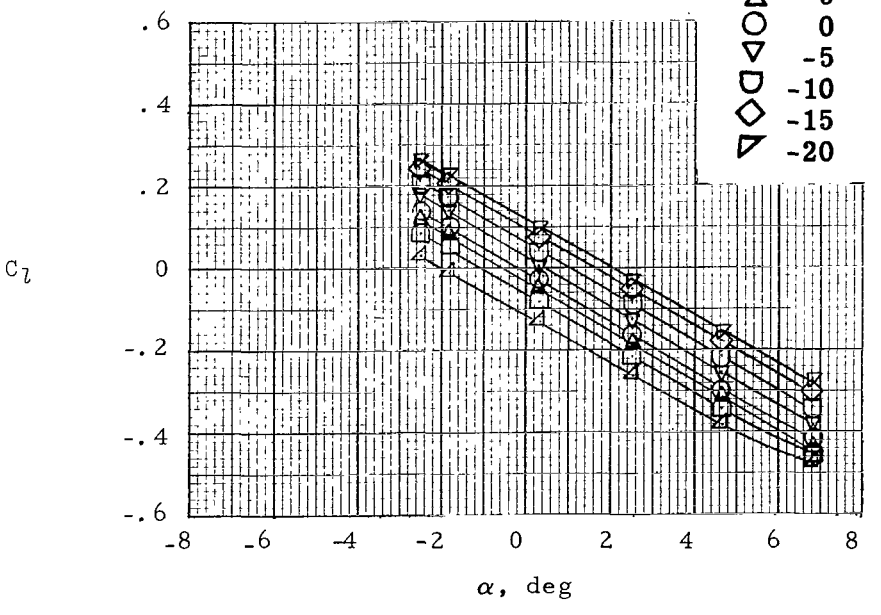

(j) M = 1.90.

Figure 6.- Continued.

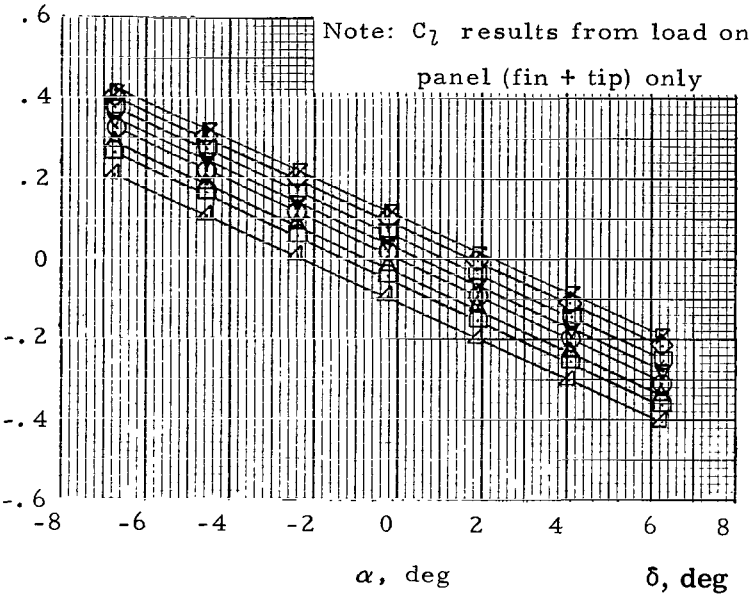

(k) M = 2.30.

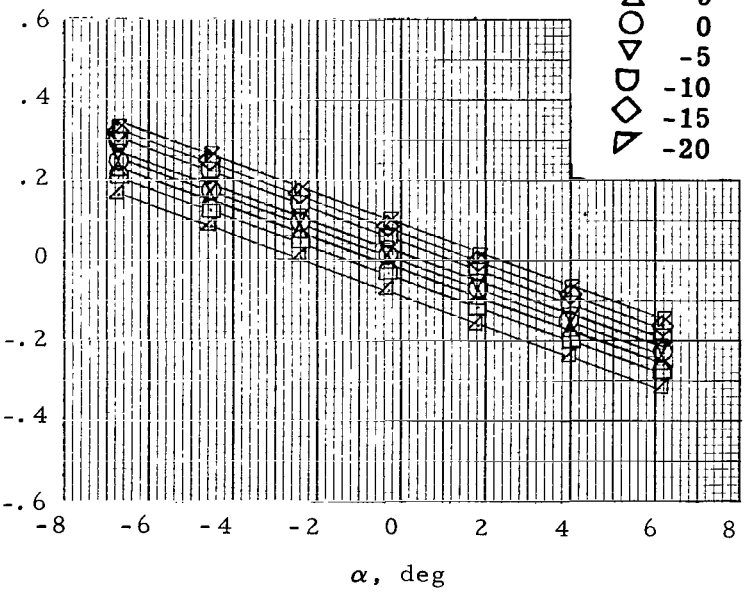

(l) M = 2.96.

Figure 6.- Continued.

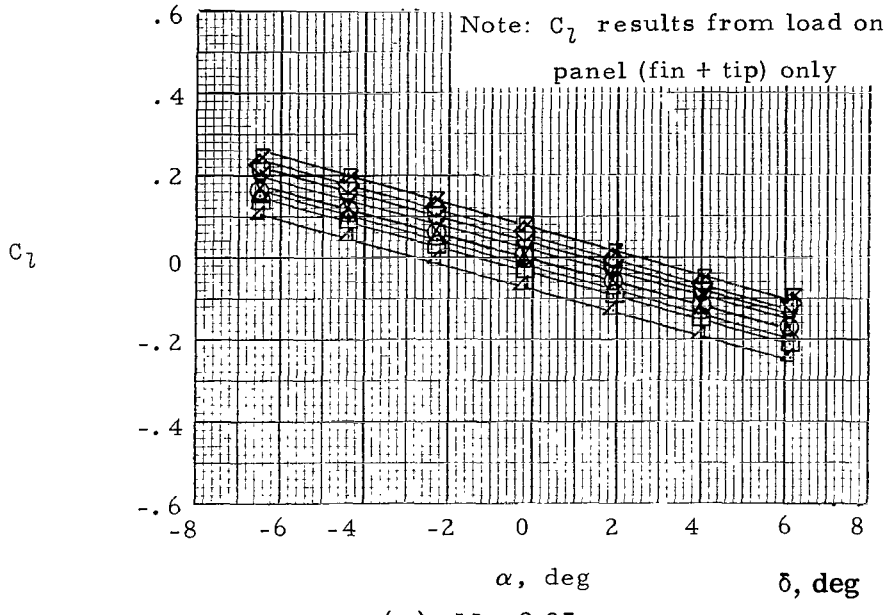

(m) M = 3.95.

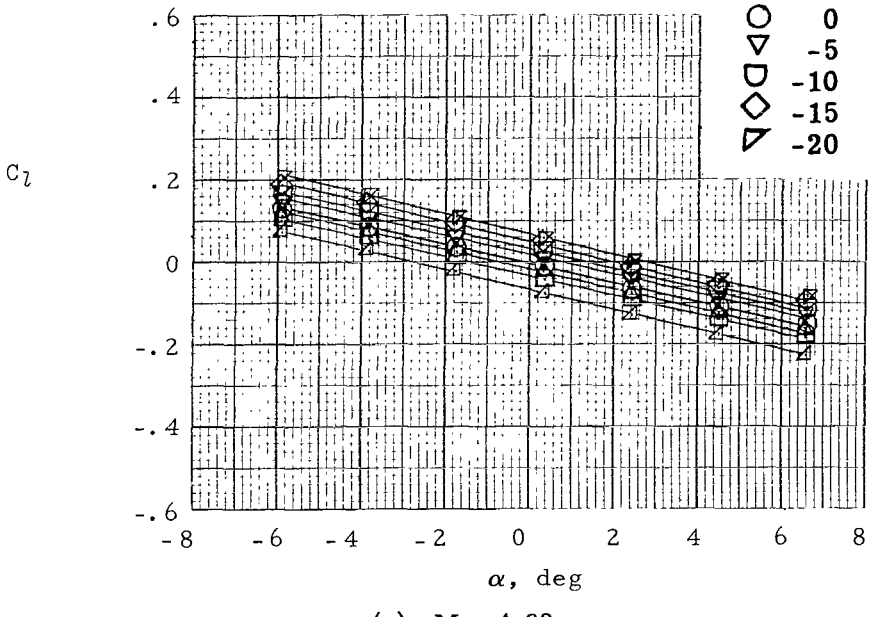

(n) M = 4.63.

Figure 6.- Concluded.

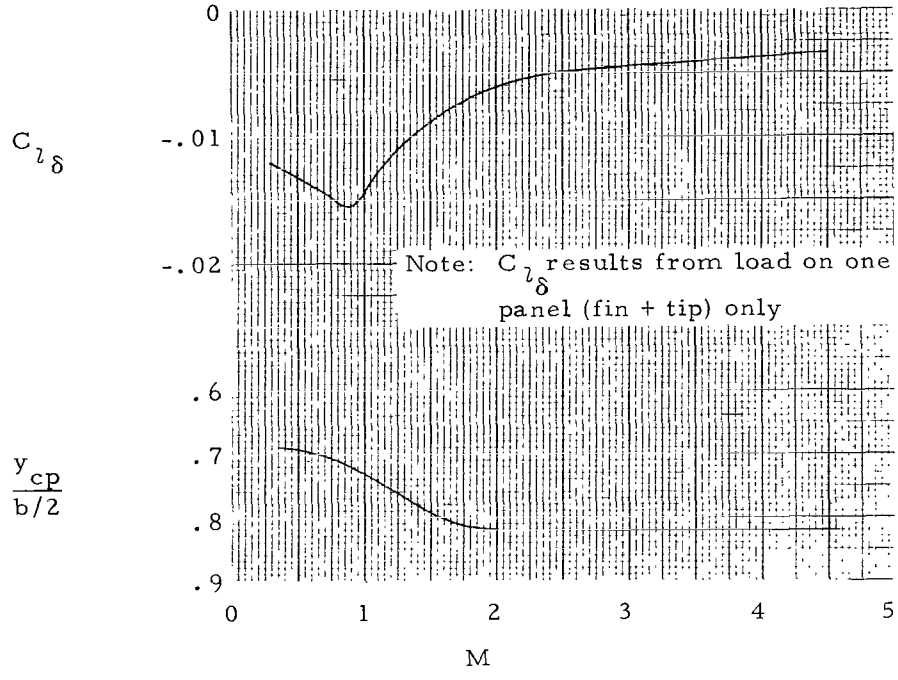

Figure 7.- Summary of roll control effectiveness of one fin tip control.

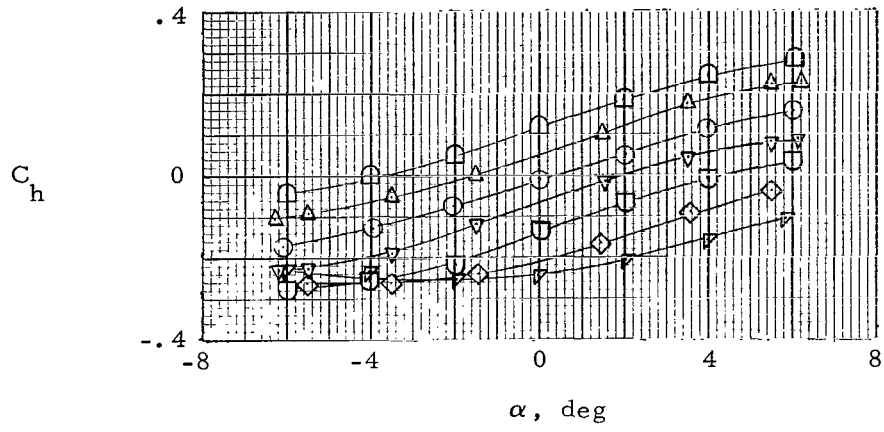

(a) M = 0.40.

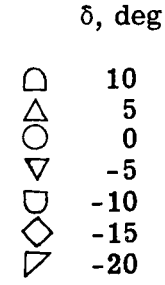

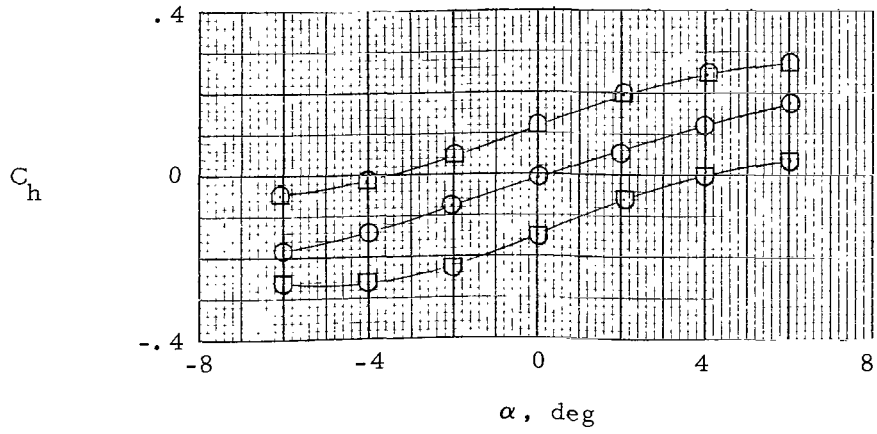

(b) M = 0.59.

Figure 8.- Enlarged fin tip control hinge-moment coefficient. $\phi = 0^{o}$.

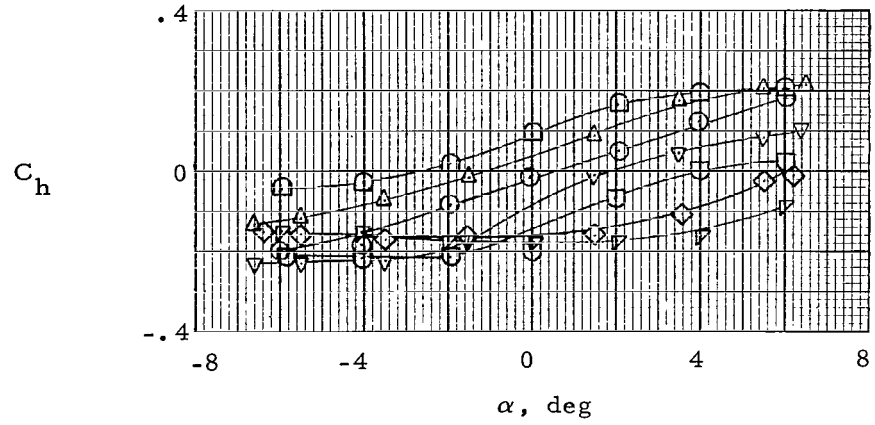

(c) M = 0.81.

δ, deg

10
5
0
-5
-10
-15
-20

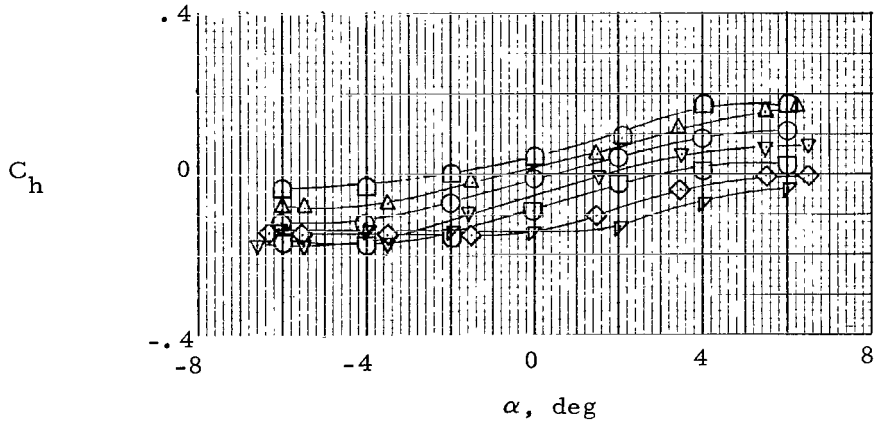

(d) M = 0.90.

Figure 8.- Continued.

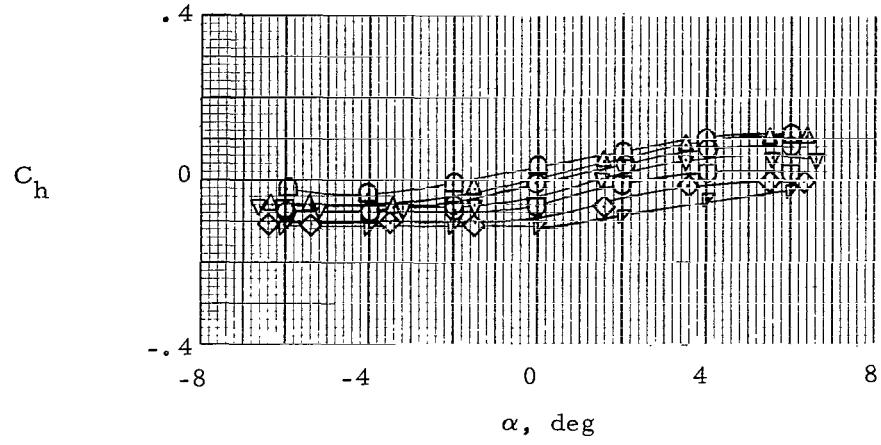

(e) M = 1.00.

δ, deg

⊓	10
△	5
○	0
▽	-5
⊔	-10
◇	-15
▽	-20

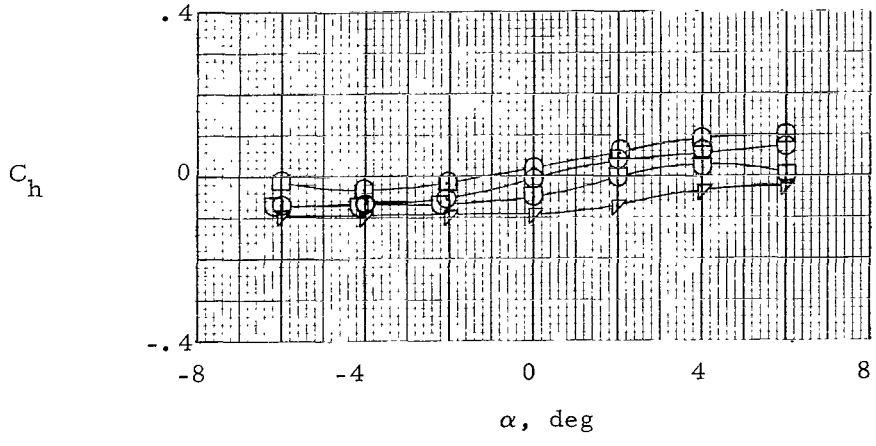

(f) M = 1.10.

Figure 8.- Continued.

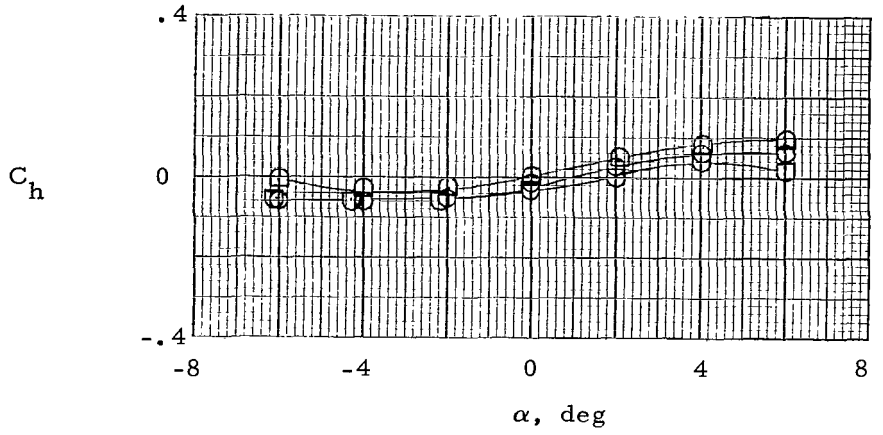

(g) M = 1.20.

δ, deg

10
5
0
-5
-10
-15
-20

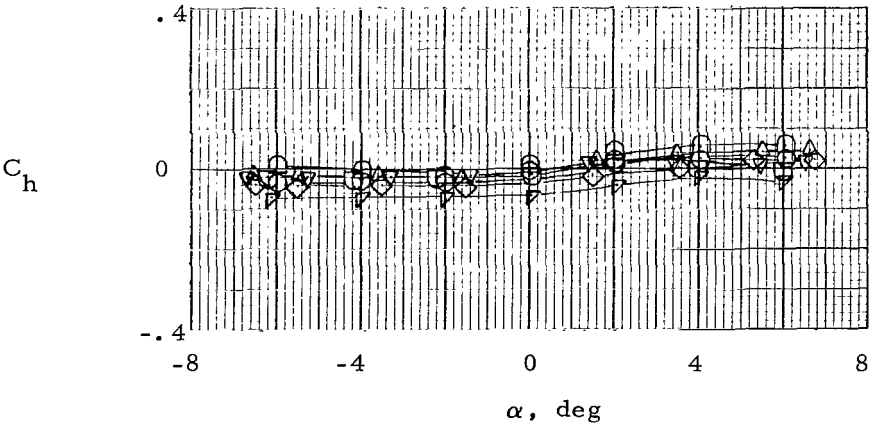

(h) M = 1.39.

Figure 8.- Continued.

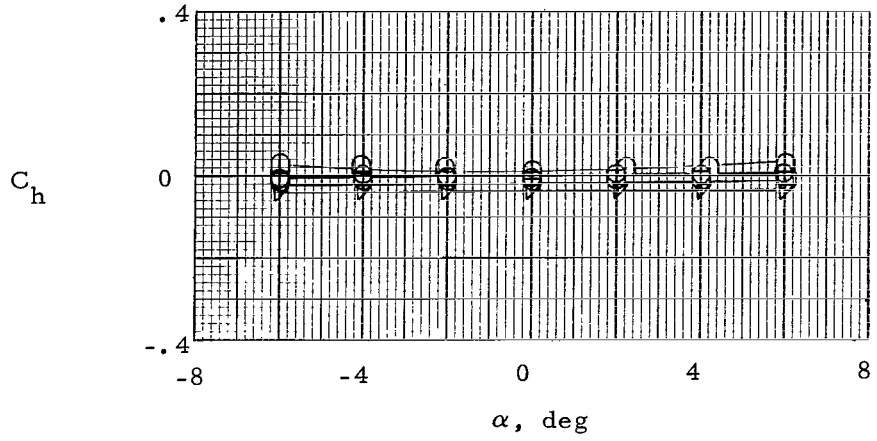

(i) M = 1.63.

δ, deg

◁	20
□	10
△	5
○	0
▽	-5
▢	-10
◇	-15
▽	-20

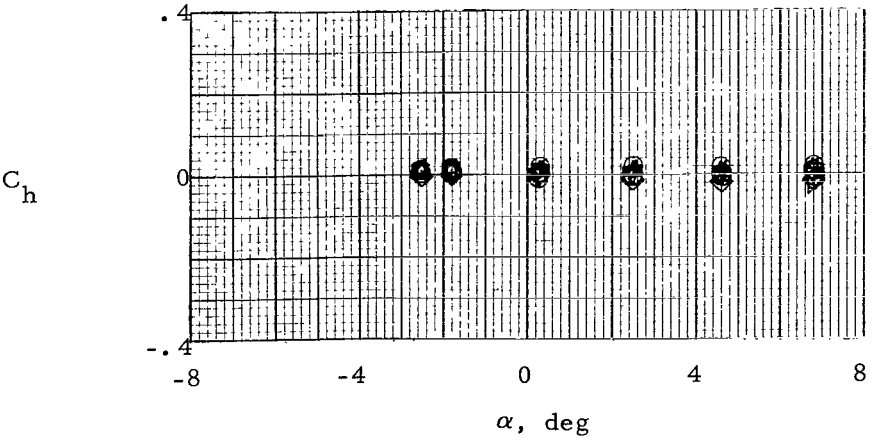

(j) M = 1.90.

Figure 8.- Continued.

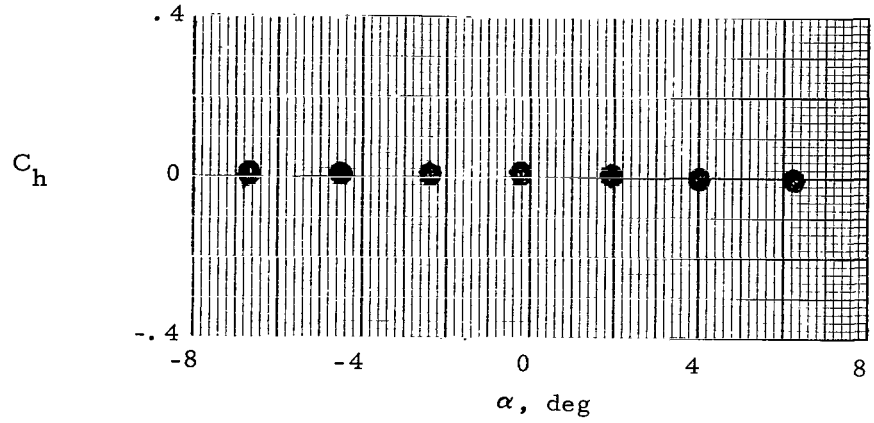

(k) M = 2.30.

δ, deg

20
10
5
0
-5
-10
-15
-20

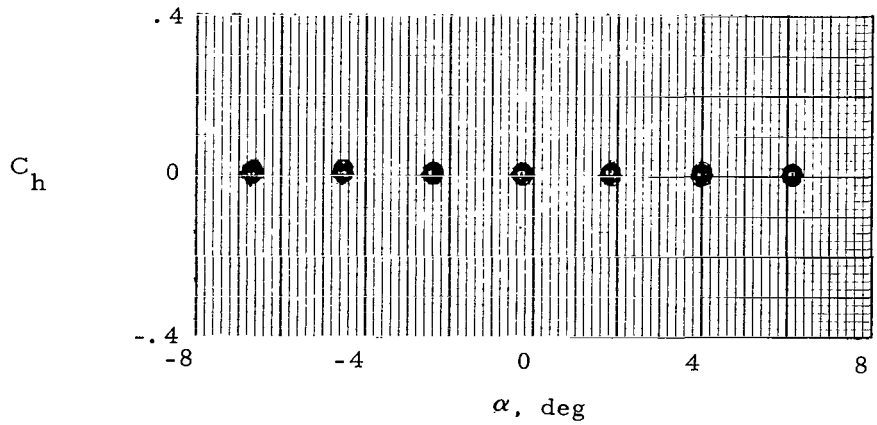

(l) M = 2.96.

Figure 8.- Continued.

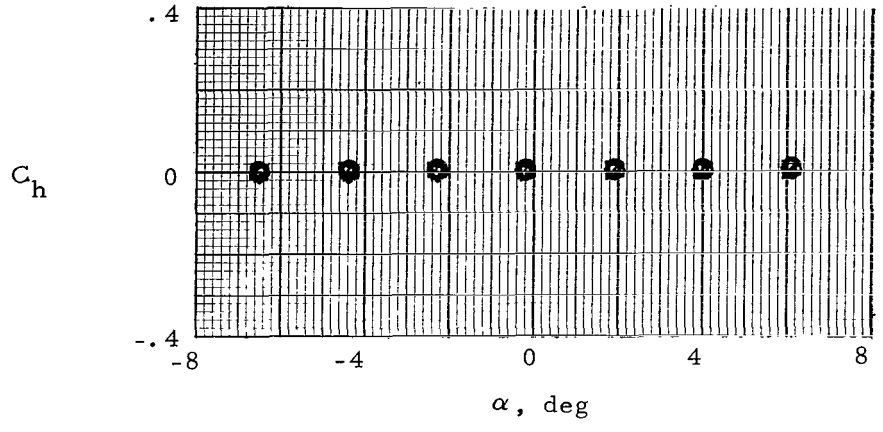

(m) M = 3.95.

δ, deg

20
10
5
0
-5
-10
-15
-20

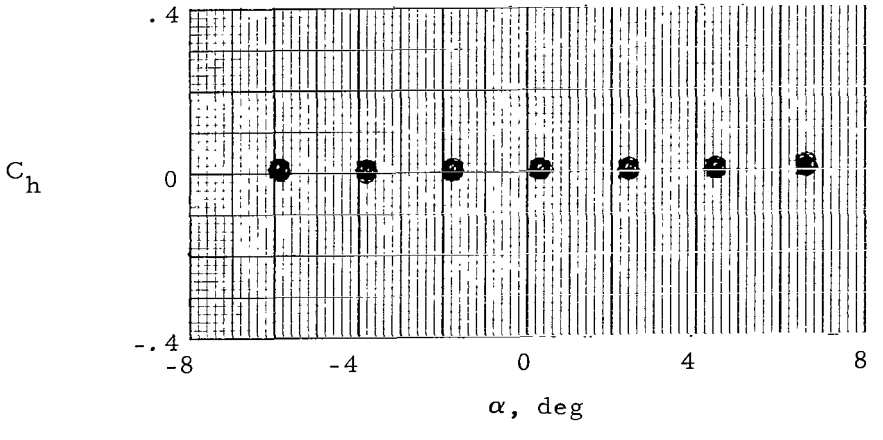

(n) M = 4.63.

Figure 8.- Concluded.

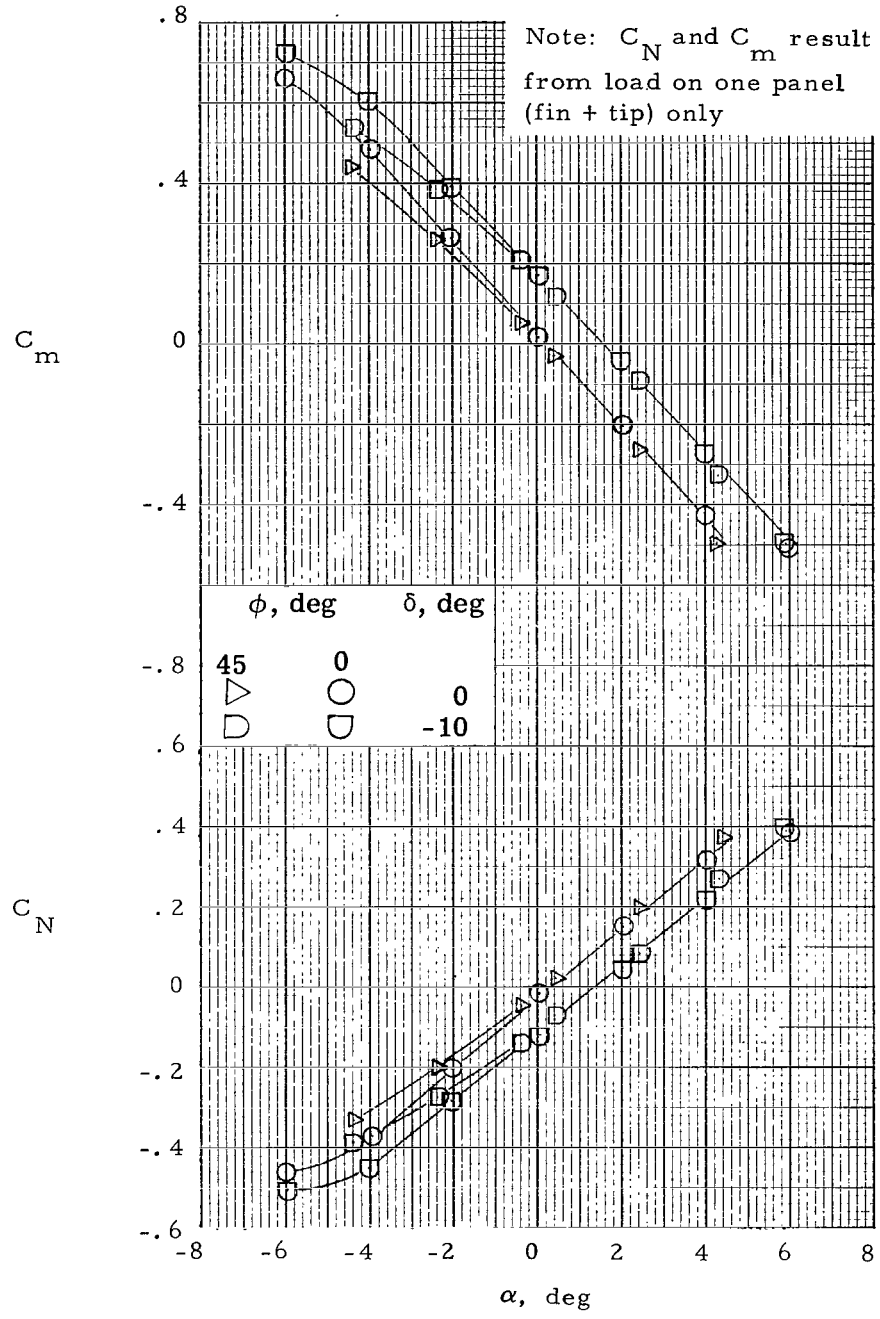

Figure 9.- Stability and control characteristics of fin at M = 1.00. $\phi = 0^o$ and 45^o; $\delta = 0^o$ and -10^o.

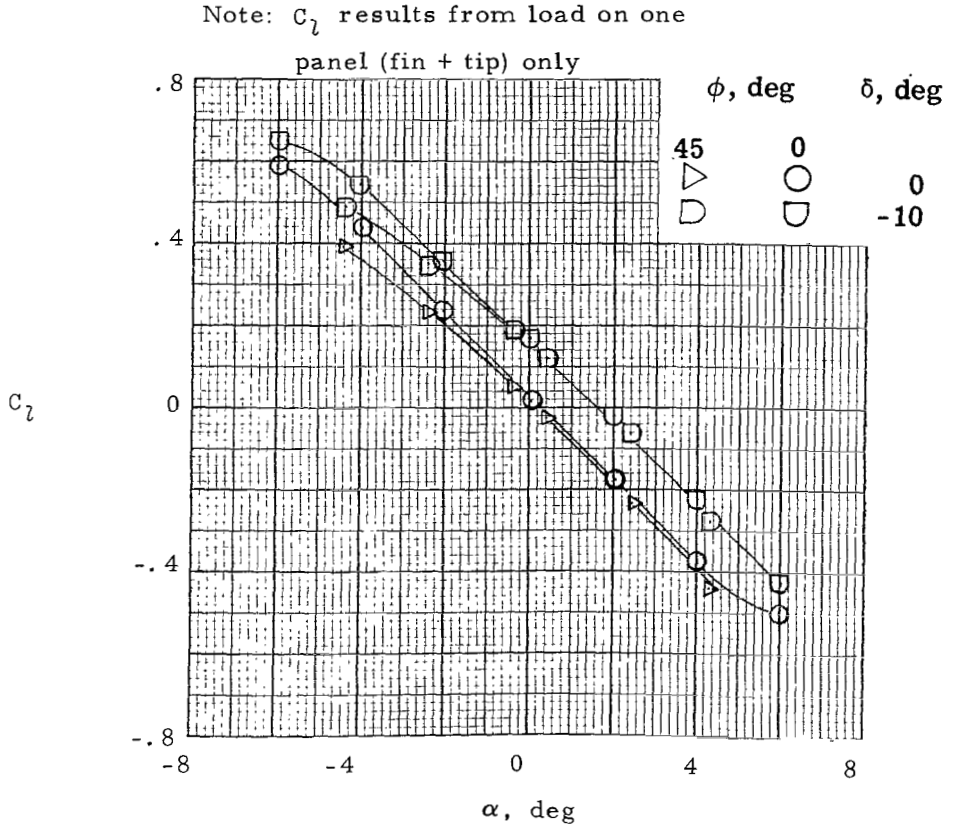

Figure 10.- Fin rolling-moment coefficient at M = 1.00. $\phi = 0^{\circ}$ and 45°; $\delta = 0^{\circ}$ and -10°.

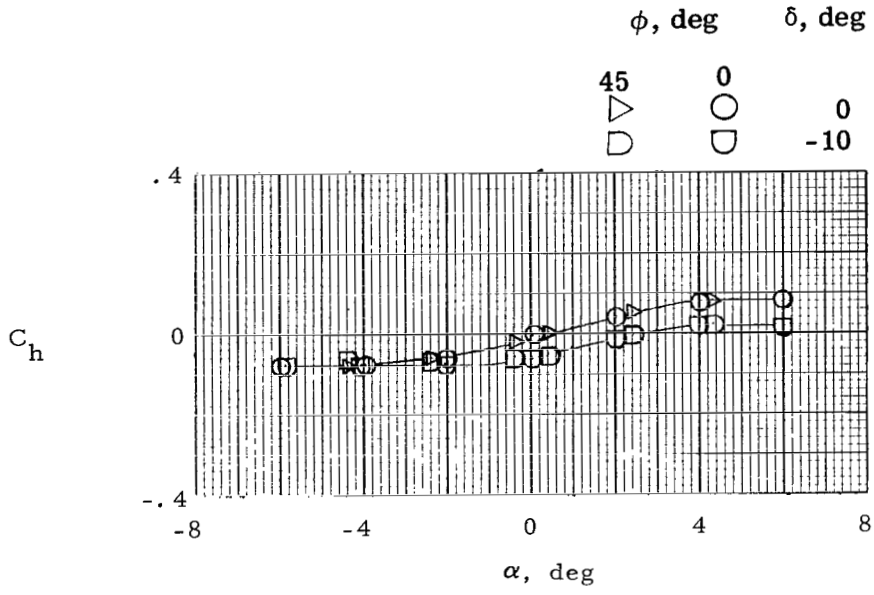

Figure 11.- Enlarged fin tip control hinge-moment coefficient at M = 1.00. $\phi = 0^o$ and 45^o; $\delta = 0^o$ and -10^o.

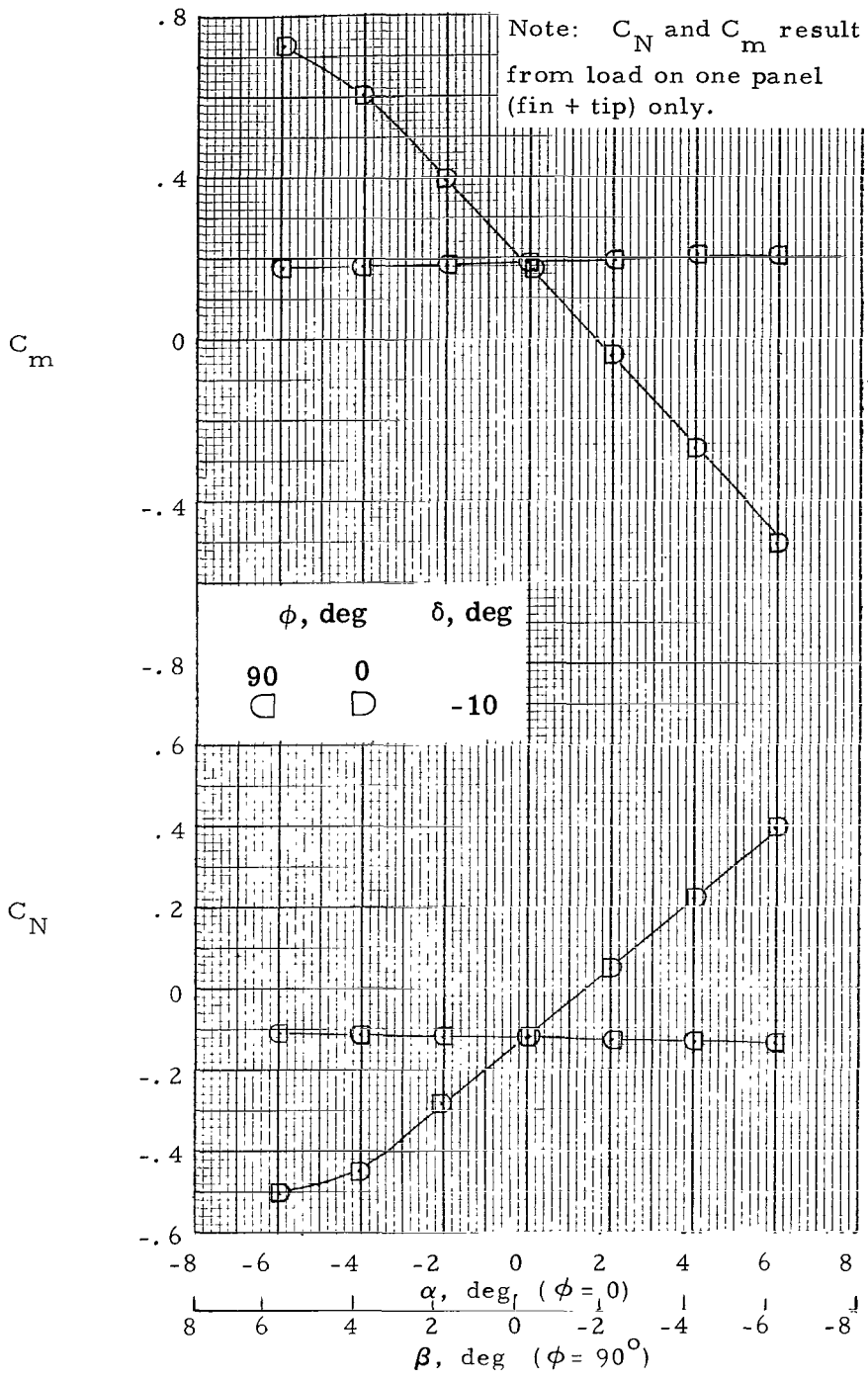

Figure 12.- Stability and control characteristics of fin at M = 1.00. $\phi = 0^{\circ}$ and 90°; $\delta = -10^{\circ}$.

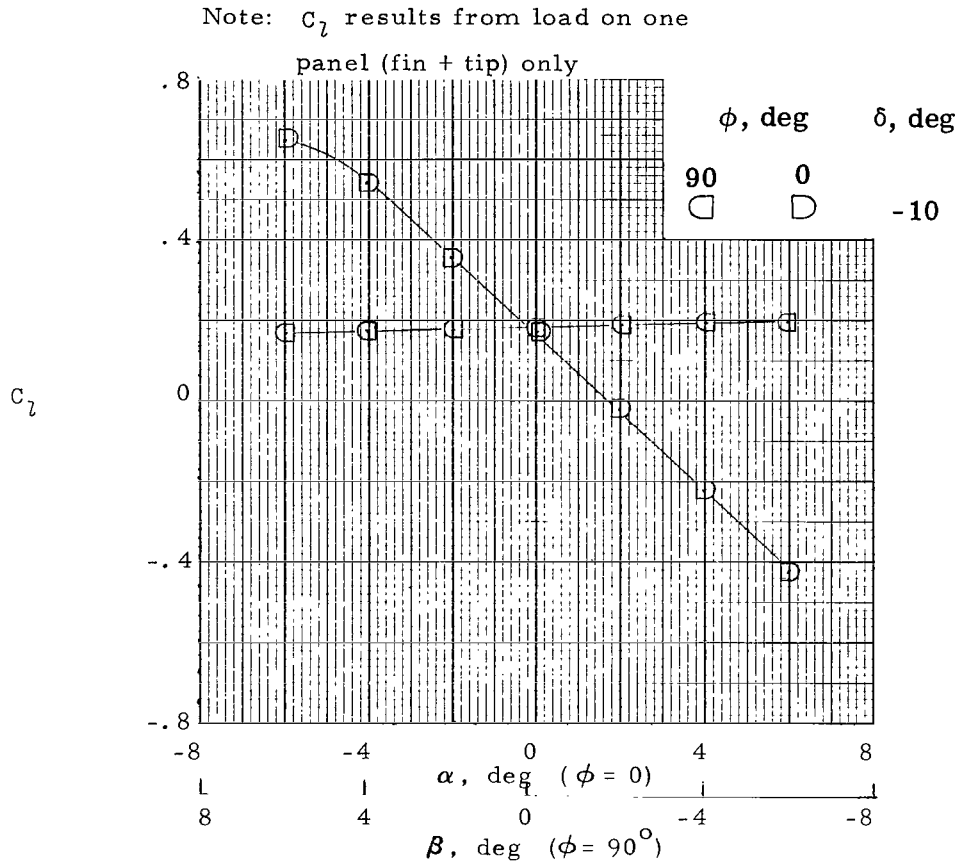

Figure 13.- Fin rolling-moment coefficient at M = 1.00. $\phi = 0^{o}$ and 90^{o}; $\delta = -10^{o}$.

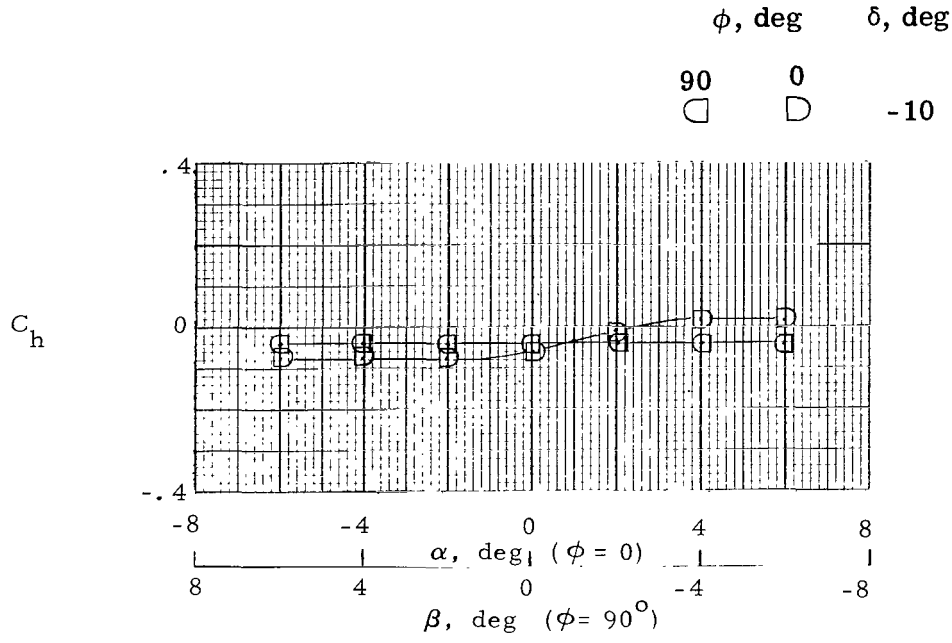

Figure 14.- Enlarged fin tip control hinge-moment coefficient at M = 1.00. $\phi = 0^{o}$ and 90^{o}; $\delta = -10^{o}$.

NASA-Langley, 1971 — 31 L-7680

"The aeronautical and space activities of the United States shall be conducted so as to contribute . . . to the expansion of human knowledge of phenomena in the atmosphere and space. The Administration shall provide for the widest practicable and appropriate dissemination of information concerning its activities and the results thereof."

—NATIONAL AERONAUTICS AND SPACE ACT OF 1958

NASA SCIENTIFIC AND TECHNICAL PUBLICATIONS

TECHNICAL REPORTS: Scientific and technical information considered important, complete, and a lasting contribution to existing knowledge.

TECHNICAL NOTES: Information less broad in scope but nevertheless of importance as a contribution to existing knowledge.

TECHNICAL MEMORANDUMS: Information receiving limited distribution because of preliminary data, security classification, or other reasons.

CONTRACTOR REPORTS: Scientific and technical information generated under a NASA contract or grant and considered an important contribution to existing knowledge.

TECHNICAL TRANSLATIONS: Information published in a foreign language considered to merit NASA distribution in English.

SPECIAL PUBLICATIONS: Information derived from or of value to NASA activities. Publications include conference proceedings, monographs, data compilations, handbooks, sourcebooks, and special bibliographies.

TECHNOLOGY UTILIZATION PUBLICATIONS: Information on technology used by NASA that may be of particular interest in commercial and other non-aerospace applications. Publications include Tech Briefs, Technology Utilization Reports and Technology Surveys.

Details on the availability of these publications may be obtained from:

SCIENTIFIC AND TECHNICAL INFORMATION OFFICE

NATIONAL AERONAUTICS AND SPACE ADMINISTRATION

Washington, D.C. 20546